Characterizing the Inflammatory Role of the Short-Chain Fatty Acid Butyrate in Macrophages

Doctoral thesis

to obtain a doctorate (Dr. med.)

from the Faculty of Medicine

of the University of Bonn

Antonia Wagener

from Waldbröl

2026

Written with authorization of
the Faculty of Medicine of the University of Bonn

First reviewer: Prof. Dr. Eicke Latz

Second reviewer: Prof. Dr. Achim Hörauf

Day of oral examination: 09.02.2026

From the institute of Innate Immunity

„Zwei Dinge sollen Kinder von ihren Eltern bekommen: Wurzeln und Flügel.“
(Johann Wolfgang von Goethe)

Für meine verstorbene Mutter, in ewiger Dankbarkeit.

Table of Contents

List of abbreviations **8**
1 Introduction **11**
1.1 An overview of the immune system 11
1.1.1 Pathogen recognition receptors and their recognition mechanisms 12
1.1.2 The IL-10 pathway 13
1.2 Gut immunity 15
1.2.1 Structure and function of the intestinal barrier 15
1.2.2 Intestinal macrophages and their role in immune tolerance 16
1.3 Short-chain fatty acids 17
1.3.1 Commensal bacteria and their fermentation products 17
1.3.2 SCFAs: Classification and functions 17
1.3.3 Impact of SCFAs on histone deacetylases 19
1.4 Inflammatory bowel disease 20
1.4.1 Genetical predisposition 21
1.4.2 Environmental factors 22
1.4.3 Immune response dysregulation 22
1.4.4 Therapeutic approaches for IBD 23
1.5 Objective 23
2 Materials and methods **25**
2.1 Materials 25
2.1.1 Devices 25
2.1.2 Consumables 26
2.1.3 Chemicals and Reagents 26
2.1.4 Kits 28
2.1.5 Antibodies 29
2.1.6 siRNAs for electroporation 30
2.1.7 qPCR primers 30
2.1.8 Cell culture media 31
2.1.9 Buffers and Solutions 31
2.1.10 Primary cells 32
2.2 Methods 32

2.2.1 Cell culture and counting 33
2.2.2 Purification and differentiation of primary human monocyte-derived macrophages 33
2.2.3 HDAC knockdown by small interfering RNA in primary human macrophages 34
2.2.4 Stimulation of primary human monocyte derived macrophages 35
2.2.5 HDAC inhibitor experiments in primary human macrophages 35
2.2.6 Homogenous Time Resolved Fluorescence 37
2.2.7 mRNA expression level analysis 37
2.2.8 Western blot and Simple Western assay on WES™ 38
2.2.9 Chromatin Immunoprecipitation sequencing (ChIP-seq) 41
2.2.10 Statistical Analysis 42
3 Results 43
3.1 The impact of single HDAC knockdown in primary human macrophages 43
3.2 The impact of HDAC inhibitors on IL-10 levels in primary human macrophages 46
3.3 Butyrate blocks IL-10 expression on transcriptional level in primary human macrophages 49
3.4 Impact of HDAC1-3 knockdown on LPS-induced IL-10 signaling in primary human macrophages 51
3.5 Butyrate inhibits STAT3 phosphorylation via HDAC inhibition 53
3.6 Acetylation status of the IL-10 gene locus 55
4 Discussion 56
4.1 Butyrate exerts pro-inflammatory effects on GM-CSF macrophages in a TLR4-dependent manner 56
4.2 Pro-inflammatory effect of butyrate depends on HDAC Inhibition in GM-CSF macrophages 57
4.3 Butyrate acts pro-inflammatory via class I HDAC inhibition in GM-CSF macrophages 58
4.4 Butyrate blocks nuclear and mitochondrial STAT3 phosphorylation 60
4.5 Limitations of the experimental approach and future perspective 61
4.6 Conclusion 62
5 Summary 64
6 List of figures 66

7 List of tables **67**

8 References **68**

9 Statement on own contribution **85**

10 Publications **86**

11 Acknowledgments **87**

List of abbreviations

AIM2	Absent in melanoma 2
ALR	Absent in melanoma 2 (AIM2)-like receptor
AMP	Antimicrobial protein
ANOVA	Analysis of variance
APC	Antigen-presenting cell
ATP	Adenosine triphosphate
BCA	Bicinchoninic acid
BSA	Bovine serum albumin
C2	Acetate
C3	Propionate
C4	Butyrate
CD	Crohn's disease
CD	Cluster of Differentiation
cDNA	complementary DNA
ChIP	Chromatin immunoprecipitation
CLR	C-type lectin receptor
COX2	Cyclooxygenase 2
CPB	Cycles per burst
DAMP	Damage-associated molecular pattern
DC	Dendritic cell
DNA	Deoxyribonucleic acid
FCS	Fetal calf serum
GIT	Gastrointestinal tract
GM-CSF	Granulocyte-monocyte colony-stimulating factor
GPCR	G-protein-coupled receptor
GWAS	Genome-wide association study
H3K27	Histone 3 Lysine 27
H3K27ac	Histone 3 Lysine 27 acetylation
HAT	Histone acetyltransferase
HDAC	Histone deacetylase

HDACi	HDAC inhibitor
hMDMs	Human monocyte-derived macrophages
HPRT	Hypoxanthine-guanine phosphoribosyltransferase
HSP	Heat shock protein
HTRF	Homogenous time-resolved fluorescence
IBD	Inflammatory bowel disease
IBS	Irritable bowel syndrome
IEC	Intestinal epithelial cell
IFN	Interferon
IL	Interleukin
JAK1	Janus Kinase 1
LDS	Lithium dodecyl sulfate
LPS	Lipopolysaccharide
MCT1	Monocarboxylate transporter 1
MHC	Major histocompatibility complex
mRNA	messenger RNA
NAD^+	Nicotinamide adenine dinucleotide
NK cells	Natural killer cells
NLR	Nucleotide-binding oligomerization domain receptor
NO	Nitric oxide
NOD	Nucleotide-binding oligomerization domain
Olfr78	Olfactory receptor 78
PAMP	Pathogen-associated molecular pattern
PBMC	Peripheral blood mononuclear cell
PBS	Phosphate-buffered saline
PIP	Peak incident power
PMSF	Phenylmethylsulfonyl fluoride
PRR	Pattern recognition receptors
PVDF	Polyvinylidene Fluoride
qPCR	Reverse transcription quantitative real-time PCR
RA	Rheumatoid Arthritis

rhGM-CSF	recombinant human granulocyte macrophage colony stimulating factor
RIG-1	Retinoic acid-inducible gene 1
RLR	RIG-1-like receptor
RNA	Ribonucleic acid
ROS	Reactive oxygen species
SAHA	Vorinostat
SCFA	Short chain fatty acid
SEM	Standard error of the mean
SH2	Src homology 2
sIgA	Secretory immunoglobulin A
siRNA	Small interfering RNA
Sirt	Sirtuine
SMCT1	Sodium-coupled monocarboxylate transporter 1
SOCS3	Suppressor of cytokine signaling 3
STAT3	Signal transducer and activator of transcription 3
T_{reg}	Regulatory T cell
TGF-β	Transforming growth factor β
TLR	Toll-like receptor
TNF-α	Tumor necrosis factor α
TSS	Transcription start site
TYK2	Tyrosine Kinase-2
UC	Ulcerative colitis
UKB	University Hospital Bonn
VEO-IBD	Very early onset IBD

1 Introduction

1.1 An overview of the immune system

The immune system is a complex network of organs, cells, and molecules that act synergistically to defend the human body against harmful agents such as cancer cells, toxins, and pathogens including bacteria, viruses, and fungi. It comprises two separate, but highly intertwined subsystems, the innate and adaptive immune system, ensuring optimal defense while maintaining self-tolerance (Iwasaki and Medzhitov, 2015; Riera Romo et al., 2016). The innate immune system, as the body's first line defense mechanism, is primarily activated upon encountering pathogens that penetrate physical barriers of the body. It provides rapid, non-specific protection preventing an initial spread of the intruder. The adaptive immune system establishes and improves in the course of life when the innate immune response is insufficient to control an infection, specifically targeting and facilitating the pathogens' clearance (Marshall et al., 2018).

Innate immunity serves to protect from, recognize and respond to pathogens and danger signals by a variety of defensive biological barriers. Surface epithelia that are in constant contact with the external environment such as the skin and the mucosal lining of the gastrointestinal, respiratory, or urogenital tract provide physical barriers. Next to that, human body fluids constitute chemical barriers including, tears, gastric juice, and intestinal mucus. Besides these passive protection mechanisms, the colonization with commensal microorganisms like non-pathogenic bacteria on surface epithelia prevents pathogens from crossing the surface barriers (Littman and Pamer, 2011). Innate immune cells represent a central element in innate immunity that are grouped based on their roles in immune response such as phagocytes (macrophages, neutrophils, dendritic cells (DCs)), cytotoxic effector cells (natural killer (NK) cells) and granulocytes (neutrophils, eosinophils, basophils and mast cells). They are strategically localized in the blood and reside in various solid tissues, forming a vigilant network ready to detect and respond to potential threats. Upon breaching a surface barrier, innate immune cells detect, engulf, and neutralize the pathogen in a process called phagocytosis while secreting cytokines and chemokines as messenger molecules to attract more immune cells to the site of infection.

The adaptive immune system is specialized in identifying and targeting specific antigens, enabling a more precise and tailored immune response for enhanced pathogen defense and memory formation, while collaborating with the innate immune system to optimize overall immune effectiveness (Flajnik and Kasahara, 2010).

The key effector cells of the adaptive immune system are two types of lymphocytes – B cells and T cells. Once activated by an antigen, B cells differentiate into either plasma cells for the production of specific antibodies to neutralize and clear invading pathogens, or into long-lived memory B cells that provide rapid and enhanced responses to re-exposure to the same pathogen (Hoffman et al., 2016).

T cells are further subdivided into four groups of cells. Cytotoxic T cells (Cluster of Differentiation (CD) 8^+ T cells) eliminate abnormal or infected host cells, particularly those infected with intracellular pathogens such as viruses, through direct cell-to-cell contact and release of cytotoxic granules (Cassioli and Baldari, 2022). Helper T cells ($CD4^+$ T cells) are activated by antigen-presenting cells (APCs), such as dendritic cells or macrophages, which present processed microbe-derived peptides on their surface using major histocompatibility complex class II (MHC-II) molecules. $CD4^+$ T cells then help regulate the immune responses by releasing cytokines that support the activities of other immune cells, such as B cells and cytotoxic T cells (Luckheeram et al., 2012). Regulatory T cells (T_{reg}) suppress excessive immune responses while maintaining self-tolerance and preventing autoimmune diseases (Kondelkova et al., 2010). Similar to memory B cells, memory T cells retain antigen recognition and provide rapid and robust responses upon reinfections with the same pathogen (Mueller et al., 2013).

1.1.1 Pathogen recognition receptors and their recognition mechanisms

Pathogen-associated molecular patterns (PAMPs) are evolutionarily highly conserved molecular motifs consisting of carbohydrates, lipoproteins, and nucleic acids found on the surfaces or structures of pathogens such as bacteria, viruses, and fungi (Zindel and Kubes, 2020). Lipopolysaccharide (LPS) from the surface of gram-negative bacteria is one of the most prominent representatives of PAMPs. PAMPs bind to and activate pattern recognition receptors (PRRs) on innate immune cells initiating intracellular signaling cascades, that trigger proinflammatory and antimicrobial responses (Mogensen, 2009). In addition to PAMPs, sterile inflammation triggers the release of endogenous molecules

called damage-associated molecular patterns (DAMPs) from damaged or stressed cells, which are also sensed by PRRs (Chen and Nunez, 2010). DAMPs include heat shock proteins (HSPs), adenosine triphosphate (ATP), and uric acid (Bours et al., 2006; Kono et al., 2010; Quintana and Cohen, 2005).

Germline-encoded PRRs consist of a group of receptors that sense PAMPs and DAMPs both extracellularly and intracellularly (Chuenchor et al., 2014; Motta et al., 2015). Based on their protein domain homology, PRRs are subdivided into five classes: Toll-like receptors (TLRs), nucleotide-binding oligomerization domain (NOD)-receptors (NLRs), retinoic acid-inducible gene 1 (RIG-1)-like receptors (RLRs), C-type lectin receptors (CLRs), and absent in melanoma-2 (AIM2)-like receptors (ALRs) (Li and Wu, 2021). They differ primarily in the molecular structures they recognize and are expressed both on immune and non-immune cells (Kawai and Akira, 2009).

One of the key PRRs that is expressed by macrophages to detect bacterial infections is TLR4. TLR4 is a transmembrane protein that plays a crucial role in detecting the presence of pathogens by recognizing LPS from the outer membranes of gram-negative bacteria. Upon LPS binding, TLR4 activates signaling pathways that lead to the production of mainly pro-inflammatory cytokines and chemokines, initiating an immune response against the invading pathogens.

As a result of TLR4 pathway activation, pro-inflammatory mediators such as tumor necrosis factor α (TNF-α), interleukin (IL)-6, cyclooxygenase 2 (COX2), and type I and III interferons are produced (Kawai and Akira, 2011; Kawai et al., 2001; Meissner et al., 2013). To prevent an excessive inflammation and to maintain immune homeostasis, anti-inflammatory molecules such as IL-10 are also induced (Chang et al., 2007; Chanteux et al., 2007; Meissner et al., 2013). IL-10 in turn leads to a feedback inhibition of inflammation-promoting cytokines, preventing immune over-activation and limiting tissue damage (Iyer and Cheng, 2012).

1.1.2 The IL-10 pathway

Interleukin 10 (IL-10) is an essential anti-inflammatory cytokine highly important in regulating overshooting immune responses and autoimmune diseases. It is produced both by innate and adaptive immune cells such as macrophages, dendritic cells, NK cells, B cells, and $CD4^+$ T cells (Iyer and Cheng, 2012). The corresponding IL-10 receptor is a

heterotetrameric complex composed of two ligand-binding domains IL-10Rα (IL-10R1) and two signaling subunits IL-10Rβ (IL-10R2) (Figure 1) (Kotenko et al., 1997; Tan et al., 1993). It is expressed by most hematopoietic cells, with monocytes and macrophages being the primary target of IL-10 (Iyer and Cheng, 2012). Upon binding of IL-10 dimers to its extracellular receptor domain IL-10Rα, the tyrosine kinases Janus Kinase-1 (Jak1) and Tyrosine Kinase-2 (Tyk2) associated with IL-10Rα and IL-10Rβ, respectively, are phosphorylated and activated. The kinases in turn phosphorylate distinct tyrosine residues (Y446, Y496) on the intracellular domain of the IL-10Rα, functioning as docking site for the Src homology 2 (SH2) domain of the signal transducer and activator of transcription 3 (STAT3). STAT3 is then phosphorylated by Jak1 and Tyk2, it forms a homodimer and subsequently translocates to the nucleus where it binds with high affinity to STAT-binding elements in promoter areas of IL-10-responsive genes (Finbloom and Winestock, 1995; Murray, 2007; Williams et al., 2004). As a result, STAT3 gene products inhibit the release of pro-inflammatory cytokines at the level of transcription mainly defining the IL-10-mediated anti-inflammatory response (Murray, 2005).

Notably, STAT3 is not only the signal transducer of the anti-inflammatory IL-10 pathway but also of pro-inflammatory cytokines such as IL-6 generating contrary responses even in the same cell type (Hutchins et al., 2013; Murray, 2006). This paradox is most likely dependent on selective cofactors interacting with STAT3 leading to this distinct pattern of gene expression. One of those cofactors being induced in macrophages by STAT3 in both IL-10 and IL-6 pathways is the suppressor of cytokine signaling 3 (SOCS3), feedback inhibiting the activity of the IL-6 receptor (Croker et al., 2003; Lang et al., 2003). In contrast, the IL-10 signaling is not affected by SOCS3, maintaining STAT3 activity (Williams et al., 2004).

As a result of sustained STAT3 activation and subsequent transcriptional inhibition of genes encoding cytokines, chemokines, cell surface molecules, and other molecules required for full immune response, the IL-10/STAT3 axis is the central player in this anti-inflammatory setting (Murray, 2005). To date, it is not yet fully understood how the STAT3 activation results in the anti-inflammatory activity of IL-10.

The importance of IL-10 as a regulatory and anti-inflammatory cytokine becomes clear when there is a disruption in the IL-10 pathway leading to inflammatory and autoimmune diseases such as inflammatory bowel disease (IBD) (Iyer and Cheng, 2012).

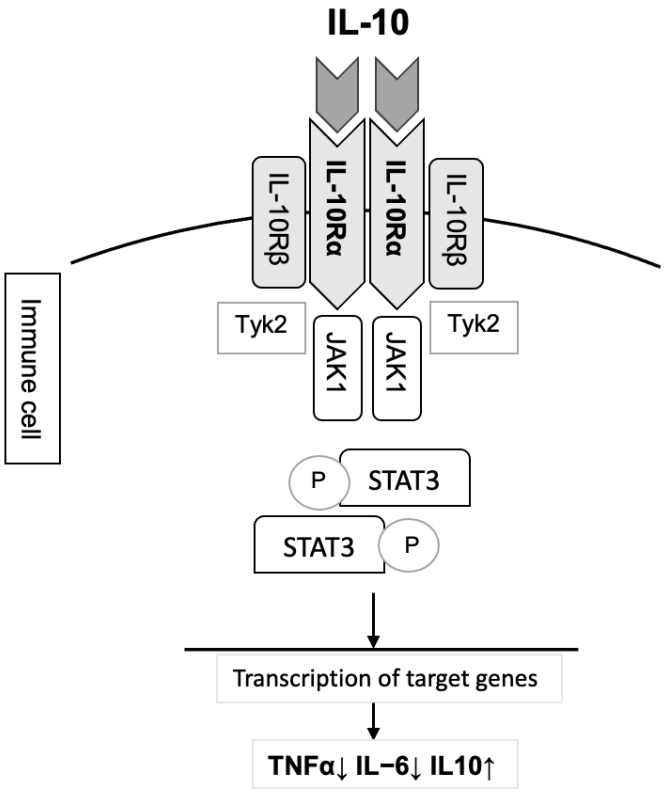

Figure 1: Diagram of the IL-10 Pathway.
Interleukin 10 (IL-10) dimer binding to the heterotetrametric IL-10 receptor leads to the phosphorylation of signal transducer and activator of transcription 3 (STAT3) by Janus Kinase-1 (JAK1) and Tyrosine Kinase-2 (Tyk2) in immune cells. STAT3 translocates to the nucleus where it induces the transcription of target genes. Figure adapted from Zhu et al. (Zhu et al., 2017)

1.2 Gut immunity

1.2.1 Structure and function of the intestinal barrier

The human gut, with the largest epithelial surface area in the body (around 200 m^2) is in constant exchange with the external environment and forms a platform that, in addition to nutrients, is also exposed to a very high number of potential pathogens. For this reason, it is important to form a well-functioning intestinal barrier, which is composed of physical and immunological elements (Vancamelbeke and Vermeire, 2017). The intestinal barrier is generally structured in multiple layers. The mucus layer that coats the inner surface of the gastrointestinal tract (GIT) harbors commensal gut microbiota as well as antimicrobial

peptides such as antimicrobial proteins (AMPs) and secretory immunoglobulin A (sIgA). Tight-junction-linked intestinal epithelial cells (IECs) form the middle layer of the intestinal barrier. In addition to providing a protective border between the gut lumen and its lamina propria, IECs are selectively permeable to water and nutrients, which is important for the gut's primary function – digestion (Gierynska et al., 2022). Next to that, IECs play an important role in the bidirectional communication of the commensal bacteria with the host immune cells (Goto, 2019). Lastly, the lamina propria, where both innate (e.g., macrophages, dendritic cells) and adaptive (e.g. B and T lymphocytes) immune cells reside, is located adjacent to the intestinal epithelial cells. (Stolfi et al., 2022)

In the face of constant environmental challenges, it is important to maintain intestinal homeostasis in which the intestinal microbiota, IECs, and the host immune system interact in a complex and sophisticated manner. Dysfunction of the intestinal barrier can result in an increased permeability, allowing pathogens, toxins, and food particles to penetrate the intestinal lining contributing to and causing various pathological conditions such as inflammatory bowel disease (IBD), irritable bowel syndrome (IBS), celiac disease, obesity and type 1 diabetes (Bosi et al., 2006; Fasano et al., 2000; Genser et al., 2018; Groschwitz and Hogan, 2009; Hanning et al., 2021; Mankertz and Schulzke, 2007; Martinez et al., 2013; Martini et al., 2017; Valitutti et al., 2019).

1.2.2 Intestinal macrophages and their role in immune tolerance

The intestinal immune system is capable of developing immune tolerance to an abundance of harmless microorganisms, while generating an adequate immune response against pathogens (Mowat, 2018). This intestinal homeostasis is mainly maintained by resident intestinal macrophages, which are the most frequent leukocytes in the lamina propria of the gut (Mowat and Agace, 2014). Unlike conventional macrophages found in other organs, intestinal macrophages attenuate systemic inflammation while promoting immune tolerance within the complex ecosystem of the GIT (Smythies et al., 2005). This prevention of bacterial hyperinflammation is achieved through cytokines such as IL-10 and transforming growth factor β (TGF-β) (Bain et al., 2013). The constitutive production and sensing of IL-10 by intestinal macrophages prevents inflammation by inhibiting the synthesis of pro-inflammatory cytokines that are triggered by stimuli such as TLR ligation (Ueda et al., 2010). In contrast, failure of macrophages to respond to IL-10 results in a

pro-inflammatory phenotype of macrophages, leading to the development of spontaneous colitis (Shouval et al., 2014; Zigmond et al., 2014).

1.3 Short-chain fatty acids

1.3.1 Commensal bacteria and their fermentation products

The human GIT is inhabited by a diverse community of microorganisms consisting of bacteria, fungi, viruses, and archaea, collectively referred to as the gut microbiota. Among them, bacteria are the most frequent representatives, with up to 10^{11} cells per gram of intestinal content and more than 1000 species (Mohajeri et al., 2018; Qin et al., 2010). Intestinal commensal bacteria are generally harmless and beneficial microorganisms that protect the host from colonization with opportunistic pathogens, produce vitamins, regulate the immune system, and metabolize indigestible food particles (e.g., complex carbohydrates), thereby supplying essential nutrients to the host (Martin et al., 2013). The host, in turn, provides a stable environment and nutrients for the bacteria to survive and proliferate (Mondot et al., 2013). The metabolized food particles also exert pleiotropic beneficial roles throughout the body by entering the systemic circulation. For example, short-chain fatty acids (SCFAs) were found to regulate immune responses next to the gut, as well as in the liver, lung, and central nervous system (Ney et al., 2023).

However, an imbalance in the composition and metabolic capacity of gut bacteria, known as bacterial dysbiosis, and associated changes in host-microbiota cross-talk and cross-regulation have been associated with the onset and progression of several diseases, including IBD. (Miyoshi and Chang, 2017; Pisani et al., 2022; Vijay and Valdes, 2022; Wilkins et al., 2019). In particular, reduced levels of bacterial metabolites, including SCFAs and vitamin B12, have been suggested as potential factors contributing to IBD (Nishida et al., 2018; Russo et al., 2019).

1.3.2 SCFAs: Classification and functions

SCFAs originate from anaerobic dietary fiber fermentation by commensal gut bacteria (Dalile et al., 2019). SCFAs are saturated carboxylic acids with an aliphatic tail of 1 to 5 carbon atoms (C1 – C5) (Table 1), the most abundant ones in the colon being acetate

(C2), propionate (C3), and butyrate (C4) in a molar ratio of 60:20:20 (Cummings et al., 1987). Specific enzymes of the commensal bacteria belonging to the *Bacteroidetes* and *Firmicutes* phylum promote the fermentation of dietary fibers and non-digestible carbohydrates to the main SCFA end products (C2, C3, C4) (Louis et al., 2014). The production of SCFAs in the gut is influenced by a variety of factors including the amount of dietary fiber intake, gut microbiota composition, microbial diversity, antibiotic intake, and physical activity (Siddiqui and Cresci, 2021).

SCFAs exert regulatory effects in two distinct ways. Once produced, the majority of SCFAs are taken up by IECs either by passive diffusion or by active transport via monocarboxylate transporter 1 (MCT1) and sodium-coupled monocarboxylate transporter 1 (SMCT1) (Dalile et al., 2019). Intracellularly, SCFAs influence gene regulation by modulating the activity of histone deacetylases (HDACs) and histone acetyltransferases (HATs) (Parada Venegas et al., 2019). This modulation leads to changes in chromosome condensation and gene expression, contributing to intestinal homeostasis and cancer protection. In addition, SCFAs bind to and activate various G-protein coupled receptors (GPCRs) such as GPR43, GPR41, GPR109A and Olfactory receptor 78 (Olfr78) (Brown et al., 2003; Le Poul et al., 2003; Thangaraju et al., 2009) thereby modulating immune responses and promoting epithelial repair (Parada Venegas et al., 2019). Among the SCFAs, butyrate especially is of high biological relevance being the major energy source for colonocytes as well as its beneficial effects on intestinal homeostasis (Siddiqui and Cresci, 2021). With its anti-inflammatory properties, butyrate regulates immune responses in the gut. This anti-inflammatory effect is mainly mediated by the inhibition of HDACs independent of GPCR signaling (Chang et al., 2014).

In disease states such as IBD, the amount of butyrate-producing bacteria is reduced and a concomitant decrease in propionate, acetate, and butyrate levels has been observed in patients' feces, indicating the significant impact of these SCFAs on gut health and their potential relevance for therapeutic intervention (Imhann et al., 2018; Marchesi et al., 2007; Santana et al., 2022).

Table 1: List of short-chain fatty acids. Adopted from (Heaney, 2020).

Carbon number	Nomenclature		Anion		Chemical structure
	Common	IUPAC	Common	IUPAC	
1	Formic acid	Methanoic acid	Formate	Methanoate	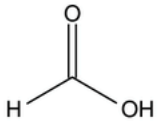
2	Acetic acid	Ethanoic acid	Acetate	Ethanoate	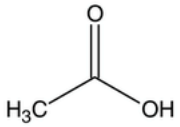
3	Propionic acid	Propanoic acid	Propionate	Propanoate	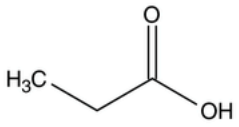
4	Butyric acid	Butanoic acid	Butyrate	Butanoate	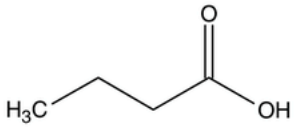
4	Isobutyric acid	2-Methylpropanoic acid	Isobutyrate	2-Methlypropanoate	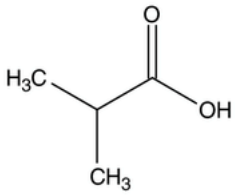
5	Valeric acid	Pentanoic acid	Valerate	Pentanoate	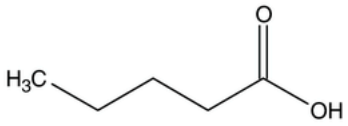
5	Isovaleric acid	3-Methylbutanoic acid	Isovalerate	3-Methylbutanoate	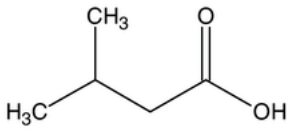
5	2-Methylbutyric acid	2-Methylbutanoic acid	2-Methylbutyrate	2-Methylbutanoate	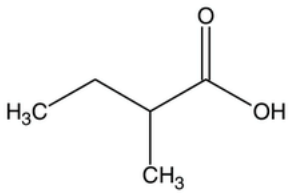

1.3.3 Impact of SCFAs on histone deacetylases

Mammalian histone deacetylases (HDACs) are enzymes responsible for the removal of acetyl groups from histone proteins in chromatin. Based on their sequence homology to yeast enzymes, HDACs are grouped into 4 principal classes (Steliou et al., 2012). Class I (HDACs 1, 2, 3, and 8), IIa (HDACs 4, 5, 7, and 9), IIb (HDACs 6 and 10), and IV (HDAC

11) HDACs are Zn^{2+} - dependent and primarily involved in histone deacetylation, whereas Class III enzymes, known as sirtuins (Sirt1-7), require Nicotinamide adenine dinucleotide (NAD^{+}) as a cofactor and are involved in a broader range of cellular processes including gene regulation, metabolism and DNA repair (Wallace and Fan, 2010). Histone deacetylation promotes gene silencing by condensing and tightening the chromatin (Huang et al., 2015; Marks et al., 2004), while histone acetylation leads to a more open chromatin configuration thus activating gene expression (Caetano and Castelucci, 2022). The biological function of HDACs is to regulate and maintain the balance of lysine acetylation levels in both histone and non-histone proteins, thereby affecting cell differentiation, metabolism, and angiogenesis (Hontecillas-Prieto et al., 2020). This reversible possibility of altering gene expression by changing the acetylation status of histones is an attractive target for cancer treatment. HDAC inhibitors (HDACi) are currently receiving much attention for their therapeutic application as potential drugs against various diseases, especially against cancer (Eckschlager et al., 2017). There are several types of HDACi, including pan-HDAC inhibitors, which simultaneously inhibit a broad range of HDAC enzymes (HDAC 1-11), and selective HDACi, which target and inhibit specific HDAC isoforms. In the gut, intrinsic HDACi activity of SCFAs such as butyrate results in epigenetic modifications that have anti-inflammatory effects by reducing macrophage activation, which contributes to immune regulation and the maintenance of gut barrier integrity (Chang et al., 2014). Interestingly, SAHA (Vorinostat) a pan-HDACi, has been shown to improve intestinal inflammation in an IBD mouse model, offering new prospects for therapeutic intervention (Glauben et al., 2006).

1.4 Inflammatory bowel disease

Inflammatory bowel disease (IBD) is a non-infectious chronic inflammation of the gastrointestinal tract (GIT), further subdivided clinically into Crohn's disease (CD), ulcerative colitis (UC) or IBD-unspecified. It has become a public health challenge with rising incidence and prevalence (> 0.3 %) not only in the Western world but also in newly industrialized countries (Ng et al., 2017). The trend from high-fiber diets to highly processed food has contributed to the rising incidence.

Although CD and UC share symptoms like diarrhea, hematochezia, and abdominal pain, they differ in terms of the affected localization of the GIT, bowel wall infiltration, and the

origin of the inflammatory lesions. CD occurs discontinuously throughout the whole gastrointestinal tract, with the terminal ileum being the most affected area, whereas UC is primarily confined to the colon (Xavier and Podolsky, 2007). Histologically, CD spreads transmurally through the intestinal wall enabling fistula formation while in UC, lesions only involve the mucosa and submucosa (Seyedian et al., 2019). Both conditions can lead to immune-related extraintestinal manifestations such as iritis, arthritis, or primary sclerosing cholangitis, significantly increasing the morbidity, mortality, and the overall burden of IBD (Sange et al., 2021). In addition, IBD may lead to the development of colorectal cancer, which has a fatal outcome in 10 to 15 % of patients with IBD, resulting from a well-described inflammation-dysplasia-carcinoma sequence (Van Der Kraak et al., 2015).
The pathogenesis of IBD is, even after decades of research, not yet completely understood; however, different etiological models exist to be relevant in the development of IBD. These models include genetic predisposition and environmental factors. An interplay of these driving factors results in an abnormal response of the mucosal immune system, which eventually leads to a chronic inflammation of the GIT.

1.4.1 Genetical predisposition

The application of genome-wide association studies (GWAS) in recent decades has significantly improved our understanding of the genetic predisposition to IBD, identifying approximately 240 loci statistically associated with susceptibility to IBD (de Lange et al., 2017; Graham and Xavier, 2020). In particular, mutations in the NOD2 gene are associated with an increased risk of IBD, particularly CD (Ashton et al., 2023).
In addition, very early-onset IBD (VEO-IBD) is correlated with polymorphisms in genes encoding IL-10 (Zhu et al., 2013), IL-10Rα, and IL-10Rβ (Moran et al., 2013), resulting in impaired IL-10 signaling and subsequent intestinal dysbiosis. In IL-10 knockout mouse models, chronic colitis developed, accompanied by morphological changes of the mucosa as well as immune alterations (Kuhn et al., 1993). Interestingly, germ-free IL-10 gene-deficient mice showed no signs of colitis, and antibiotic therapy stopped the colitis (Madsen et al., 2000), highlighting the importance of the gut microbiota in the development of IBD.

1.4.2 Environmental factors

The exposome, which includes factors such as diet, stress, environmental pollution, and medication, plays a significant role in the development and progression of IBD (Abegunde et al., 2016; Wild, 2005). In general, a high-fiber diet has been linked to a protective effect against IBD, particularly CD. In a study of IL-10-deficient mice, soluble fiber consumption reduced intestinal inflammation (Bassaganya-Riera et al., 2011), and in humans, a high dietary fiber intake, particularly from fruits and cruciferous vegetables, was related to a reduced risk of CD (Ananthakrishnan et al., 2013).

Conversely, the Western diet, characterized by high consumption of processed foods, saturated fats, sugars, and low fiber content, has been associated with an increased risk of IBD in developed countries over the past decades (Rizzello et al., 2019). In addition, the use of antibiotics leads to significant changes in the composition of the gut microbiome, contributing to an imbalance in the gut microbiota that has been linked to IBD (Nguyen et al., 2020).

1.4.3 Immune response dysregulation

Environmental factors, genetic predisposition, and dysbiosis of the gut microbiota collectively contribute to the disruption of the intestinal mucosal barrier. This disruption activates immune responses by engaging IECs. Furthermore, commensal microbiota and their metabolites can infiltrate the compromised mucosa and initiate an innate immune response by recruiting and activating macrophages, DCs, and neutrophils.

As a result, innate immune cells promote a chronic inflammatory state within the GIT by releasing a repertoire of cytokines and chemokines, including IL-1β, IL-12, IL-6, IL-23, TNF-α, and TGF-β. In addition, T cells of various subtypes (TH1, TH2, TH17, T_{reg}) are activated by these cytokines, thereby amplifying the immune response through the production of IFN-γ, IL-17, and TNF-α (Neurath, 2014).

Together, these dysregulated mucosal immune responses lead to tissue damage and the establishment of persistent intestinal inflammation, which plays a central role in the onset and manifestation of symptoms associated with IBD (Ramos and Papadakis, 2019).

1.4.4 Therapeutic approaches for IBD

Currently, there is no curative treatment for patients with IBD. Management of IBD focuses primarily on achieving and maintaining remission by reducing the underlying inflammation and controlling symptoms. Treatment of IBD typically involves either drug therapy or surgical intervention. Medications vary in their mechanisms of action and include anti-inflammatory drugs, immunosuppressants, biologics, and antibiotics. Surgical intervention is considered when drug therapy proves insufficient or when there are complications such as strictures, fistulas, or severe inflammation that do not respond to medical therapy.

One approach to treat IBD is the therapy with fibre-derived SCFAs. However, dietary fibres that induce SCFA production have yielded inconclusive results regarding the benefits in IBD due to poor tolerability (Gearry et al., 2009; Maagaard et al., 2016).

Given the recognized beneficial effects of the SCFA butyrate on intestinal barrier function, numerous studies have explored its potential as a treatment option for IBD. However, clinical trials investigating the efficacy of butyrate supplementation have yielded indecisive results, with some studies suggesting its beneficial effects for IBD patients, while others have failed to demonstrate a significant effect on intestinal inflammation, particularly in alleviating acute symptoms of IBD (Facchin et al., 2020; Scheppach, 1996; Steinhart et al., 1996; Vernero et al., 2020). In addition, small-scale trials examining the use of oral butyrate in patients with UC and CD have shown limited improvement in symptoms and intestinal histology (Salvi and Cowles, 2021). The conflicting results of these studies highlight the complexity of butyrate's role in the management of IBD and the need for further investigation into its application as a treatment option. It is evident that the interplay between the gut microbiota, butyrate, and the host immune system in the context of IBD is multifaceted and requires a more nuanced understanding.

1.5 Objective

The SCFA butyrate, a key metabolite produced by commensal gut microbiota from dietary fiber, is commonly known to have beneficial effects on the host both locally and systemically. However, the application of both fiber and butyrate itself in inflammatory conditions such as IBD with associated intestinal barrier dysfunction resulted in contradictory outcomes. Therefore, the role of the SCFA butyrate in the context of IBD under inflammatory conditions needs to be further defined and characterized.

The inflammatory response during IBD induction involves the secretion of cytokines by immune cells such as macrophages. Hence, it is important to analyze the effect of the SCFA butyrate on the cytokine secretion in macrophages under inflammatory conditions to define the detrimental impact of butyrate in IBD.

Next to that, butyrate acts as HDACi, thereby influencing gene expression and consequently cytokine production. Thus, identifying the butyrates' exact mode of action to modify cytokines in primary human macrophages under inflammatory conditions may provide insight into potential therapeutic targets for the treatment of IBD.

Given the significance of IL-10 as major anti-inflammatory cytokine and its important role in the pathogenesis of IBD, understanding the impact of butyrate in the IL-10 pathway under inflammatory conditions is of great importance.

Therefore, the principal objectives of the study are:

1. To replicate the effects of butyrate on cytokine levels through HDAC knockdown and inhibition in primary human macrophages
2. To explore the influence of the SCFA butyrate on mRNA and protein expression levels in primary human macrophages under inflammatory conditions
3. To further characterize the impact of butyrate on TLR-4 mediated IL-10 signaling pathway.

2 Materials and methods

2.1 Materials

2.1.1 Devices

Name	Supplier
- 20°C freezer	Liebherr
- 80°C freezer	ThermoScientific
4D-nucleofector® Core Unit	Lonza Bioscience
NanoDrop™ One	Thermo Fisher Scientific
4°C fridge	Liebherr
Cell counter CASY	OMNI Life Sciences
Cell incubator	SANYO Biomedical
Centrifuges	Eppendorf
Electroporator	Invitrogen
Electroporator	Lonza
Heatblock Thermomixer	Eppendorf
M220 focused ultrasonicator	Covaris
MACS multiStand	Miteny Biotec
Multichannel pipettes	Mettler Toledo
peqSTAR Thermo cycler	VWR
Pipetboy acu	Integra Biosciences
Pipettes (0.1 µl – 1 ml)	Mettler-Toledo
Plate reader SpectraMax i3	Molecular Devices
Quant Studio 6 Flex	Applied Biosystems
Scale	Sartorius
Sterile tissue culture hood	Fischer Scientific
Tissue culture microscope	Leica
WES	Protein simple
Western Blot reader Odyssey	LICOR Biosciences

2.1.2 Consumables

Name	Supplier
12-well plates for cell culture	Greiner bio-one
24-well plates for cell culture	Greiner bio-one
384-well plates for HTRF	Labomedic
384-well qPCR plate	Applied Biosystems
6-well plate Nunc delta surface (for hMDMs)	ThermoFisher
6-well plates for cell culture	Greiner bio-one
96-well plates for cell culture	Greiner bio-one
Cell scrapers	Sarstedt
Column hMDMs purification	Miltenyi Biotech
Pipet tips (0.1 µl – 1 ml)	Mettler Toledo
Pre-separation filter for hMDM purification	Miltenyi Biotech
Screw cap tube, 15 ml	Greiner bio-one
Screw cap tube, 50 ml	Greiner bio-one
Serological pipette, plugged, 10 ml	Greiner bio-one
Serological pipette, plugged, 25 ml	Greiner bio-one
Serological pipette, plugged, 5 ml	Greiner bio-one

2.1.3 Chemicals and Reagents

Name	Supplier
2-Mercaptoethanol	Sigma-Aldrich
Abexinostat (PCI-24781)	Biomol
Bovine serum albumin (BSA)	Sigma-Aldrich
CD14 MicroBeads (human)	Miltenyi Biotechnology
cOmplete EDTA-free Protease-Inhibitor Cocktail Tablets	Roche Life Science
CUDC 101 (EPS003)	Merck
Dimethyl sulfoxide (DMSO)	AppliChem
dNTP mix (10 mM)	ThermoFisher

Drosophila spike-in chromatin (53083)	Active Motif
EDTA solution 0.5 M, pH 8.0	GIBCO
Ethanol	AppliChem
Ficoll-Paque PLUS	GE Healthcare Life Sciences
Fimepinostat (CUDC-907)	Biomol
16 % Formaldehyde (w/v), Methanol-free	ThermoFisher
G Dynabeads	Invitrogen
Immobilon-FL PVDF Membrane, 0.45 µm	Merck
LMK 235 (SML1053)	Biomol
LPS ultrapure EB	Invitrogen
Mocetinostat (MGCD 0103)	Biomol
Nucleofector P3 buffer	Lonza Bioscience
NuPAGE 10 x Sample reducing agent	Invitrogen
NuPAGE 4 x LDS loading buffer (8 % LDS, 40 % glycerol, 2.04 mM EDTA, 0.88 mM SERVA Blue G, 0.7 mM phenol red, 564 mM Tris, pH 8.5)	Invitrogen
NuPAGE Mes SDS running buffer 20x	Invitrogen
NuPAGE Mops SDS running buffer 20x	Invitrogen
NuPAGE Novex 10 % Bis-Tris Protein Gels, 1.5 mm, 10 well	Invitrogen
PageRuler Plus Prestained Protein Ladder	ThermoScientific
Panobinostat	
PBS 10 x (2 g potassium chloride, 2 g potassium dihydrogen phosphate, 80 g sodium chloride, 11.5 g/l di-sodium hydrogen phosphate anhydrous)	Pan Biotech
Penicillin/streptomycin	ThermoFisher
Phospho Stop tablets	Roche
PMSF	Applichem
Protease inhibitor cocktail	Roche
Quisinostat (JNJ 26481585)	Biomol

Reducing agent 10 x (500 mM DTT)	Life Technologies
rhGM-CSF	Immunotools
RPMI1640	GIBCO
SIS-17	Biomol
Sodium Butyrate	Sigma Aldrich
Sodium chloride (NaCl)	Sigma Aldrich
Sodium deoxycholate	Sigma Aldrich
Sodium dodecyl sulfate (SDS)	Sigma Aldrich
SR-4370	Biomol
Superscript III reverse transcriptase	ThermoFisher
TMP-195	Biomol
Trichostatin A (TSA)	Merck
Tris HCL Buffer 1 M, pH 7.4	AppliChem
Triton X-100	Roth
TRIzol Reagent	Life Technologies
Tubacin	Biomol
Vorinostat (SAHA)	Biomol

2.1.4 Kits

Kit	**Supplier**
Anti-Mouse Detection Module for Jess/Wes	Biotechne
Anti-Rabbit Detection Module for Jess/Wes	Biotechne
ChIP DNA Clean & Concentrator Kit	Zymo
Human IL-10 HTRF kit	Cisibo
Human IL-1β HTRF kit	Cisibo
Human IL-6 HTRF kit	Cisibo
Human TNF-α HTRF kit	Cisibo
Maxima Tm SYBR Green/ROX qPCR Master Mix	ThermoFisher Scientific

NEBNext Ultra DNA Library Prep kit	New England Biolabs
Pierce BCA Protein Assay Kit	ThermoFisher
RNeasy Mini Kit	Qiagen

2.1.5 Antibodies

Table 2: List of primary antibodies

Antibody	**Clone**	**Dilution**	**Company**
STAT 3	9132	1:100	CST
Phospho-STAT3 (Y705)	9145	1:100	CST
Phospho-STAT3 (S727)	9134	1:100	CST
β-Actin	926-42210	1:100	Li-cor
HDAC 1	2062	1:50	CST
HDAC 2	2540	1:50	CST
HDAC 3	85057	1:50	CST
HDAC 4	7628S	1:50	CST
HDAC 5	20458S	1:50	CST
HDAC 6	7558T	1:50	CST
HDAC 7	33418S	1:50	CST
HDAC 8	66042S	1:50	CST
HDAC 9	67364-1	1:50	Proteintech
Histone 3	9715S	1:1000	CST
H3K27Ac	8173	1:1000	CST
H3K27Ac	4729	1:1000	Abcam
Spike-in antibody	61686	1:1000	Active Motif

Table 3: List of secondary antibodies used for Western blot

Antibody	**Dilution**	**Company**
Donkey anti-mouse IgG (H*L) IRDye 800CW	1:25000	Li-Cor
Donkey anti-rabbit IgG (H*L) IRDye 680 RD	1:25000	Li-Cor

2.1.6 siRNAs for electroporation

The siRNAs used in this research were bought from ThermoFisher Scientific.

Table 4: List of siRNAs used for electroporation

Target gene	**Identifier**
Negative control #1	4390843
Negative control #2	4390844
HDAC 1 #1	130749, Assay ID s73
HDAC 1 #2	130750, Assay ID s74
HDAC 3 #1	4390824, Assay ID s16876
HDAC 3 #2	4390824, Assay ID s16877
HDAC 4 #1	4392420, Assay ID s16877
HDAC 4 #2	4392420, Assay ID s18837
HDAC 5 #1	4390824, Assay ID s19462
HDAC 5 #2	4390824, Assay ID s19463
HDAC 6 #1	4390824, Assay ID s19459
HDAC 6 #2	4392420, Assay ID s19460
HDAC 7 #1	4392420, Assay ID s28335
HDAC 7 #2	4392420, Assay ID s28336
HDAC 8 #1	4390824, Assay ID s31697
HDAC 8 #2	4390824, Assay ID s31698

2.1.7 qPCR primers

Table 5: List of qPCR primers used for amplification of human genes

Target	**Sequence**
hHPRT-F	TCAGGCAGTATAATCCAAAGATGGT
hHPRT-R	AGTCTGGCTTATATCCAACACTTCG
hIL-10-F	GCCGTGGAGCAGGTGAAGA
hIL-10-R	AGTCGCCACCCTGATGTCTC

hTNF-α-F	CCCAGGCAGTCAGATCATCTTC
hTNF-α-R	TCTCTCAGCTCCACGCCATT
hIL-6-F	GTGCCTCTTTGCTGCTTTCAC
hIL6-R	GGTACATCCTCGACGGCATCT
hIL-1β-F	CTGTACCTGTCCTGCGTGTTGA
hIL-1β-R	TGGGCAGACTCAAATTCCAGCT

2.1.8 Cell culture media

Table 6: List of cell culture medium

Medium	**Composition**	
Complete RPMI	RPMI	
	FCS	10 %
	Penicillin/streptomycin	1 %
	Sodium pyruvate	1 x
	GlutaMAX	1 x
RPMI (Electroporation)	RPMI	
	FCS	10 %
	Sodium pyruvate	1 x
	GlutaMAX	1 x

2.1.9 Buffers and Solutions

Table 7: List of buffers and solutions

Application	**Buffer name**	**Composition**	
Cell lysis	RIPA lysis buffer	Tris-HCL (pH 7.4)	20 mM
		NaCl	150 mM
		EDTA	1 mM
		Triton X-100	1 %
		Glycerol	10 %
		SDS	0.1 %

		Sodium deoxycholate	1 mM
		cOmplete EDTA-free Protease inhibitor	1 x
		PMSF	0.2 mM
		Phospho STOP	1 x
hPBMC isolation	MACs buffer	PBS	1 x
		BSA	0.5 %
		EDTA	2 mM
Western blot	Transfer Buffer	TrisGlycine Buffer	1 x
		Methanol	20 %
	Blocking Buffer	TBS	1 x
		BSA	3 %
	TBST	TBS	1 x
		Tween 20	0.05 %
	TBS	TBS	1 x

2.1.10 Primary cells

The buffy coats used in this study were provided by the blood donation service of the University Hospital Bonn (UKB). Monocytes extracted from the buffy coats were supplemented with granulocyte-monocyte colony-stimulating factor (GM-CSF) yielding human monocyte derived macrophages (hMDMs).

2.2 Methods

In order to determine the effect of HDAC knockdown on the primary hMDM, $CD14^+$ monocytes were extracted from human buffy coats and differentiated into macrophages. Subsequently, HDACs were knocked down by siRNA electroporation followed by stimulation with butyrate, LPS or a combination of both. HDACi was applied to mimic the effect of butyrate on HDACs. Cytokine levels were checked by homogenous time resolved fluorescence (HTFR) and proteins were analyzed by means of WES and Western blot.

Next to that, chromatin immunoprecipitation (ChIP) was performed to investigate protein-gene interactions determining transcription factor binding sites.

2.2.1 Cell culture and counting

Primary human monocytes and monocyte-derived macrophages were cultured in 6-well tissue culture plates at a concentration of 2.0 x 10^6 cells/ml in complete RPMI 1640 and kept at 37°C, humidified, 5 %, CO_2 atmosphere. Cell quantification and viability assessment were performed using the automated CASY Cell Counter and Analyzer, based on a multi-channel system using electrical field measurements.

2.2.2 Purification and differentiation of primary human monocyte-derived macrophages

Before starting the purification protocol, scissors and waste boxes were cleaned with 70 % ethanol and placed in a fume hood. After diluting the blood in a 1:1 ratio with PBS, 35 ml of this blood/PBS mixture was gently pipetted onto 15 ml of Ficoll. Samples were centrifuged at 700 g for 20 minutes without break to generate three separate layers. Peripheral blood mononuclear cells (PBMCs) were collected from the middle layer, transferred to a new falcon and washed once with PBS. After centrifuging for 10 minutes at 350 g (9 acc; 9 brake), the supernatant was gently discarded and the cells were washed in 25 ml MACS buffer. To isolate monocytes, PBMCs were incubated with 175 µl of CD14 magnetic microbeads for 15 minutes at 4°C and then washed once with MACS buffer. LS columns were placed in a magnetic field and equipped with pre-separation filters. After wetting the filter and column with MACS buffer, cells were transferred to the pre-separation filter. Subsequently, columns were washed 3 times with 3 ml MACS buffer. Next, $CD14^+$ monocytes were eluted in 3 ml MACS buffer and washed one time with PBS. Cells were counted and diluted in complete RPMI medium to a concentration of 2 x 10^6 cells/ml. In order to ensure the differentiation of $CD14^+$ monocytes to human macrophages, 3.1 µl/ml rhGM-CSF was added. A final volume of 5 ml per well in a 6 well-plate was seeded and cells were incubated for 3 days at 37°C, 5 % CO_2.

2.2.3 HDAC knockdown by small interfering RNA in primary human macrophages

By complementary binding to mRNA of genes of interest, small interfering RNA (siRNA) triggers the degradation of the mRNA and prevents the production of the corresponding protein. This technique allows to investigate the impact of reduced gene expression on cellular processes and helps to elucidate the function of the targeted genes. I used two different siRNA-mediated knockdown techniques which are described below.

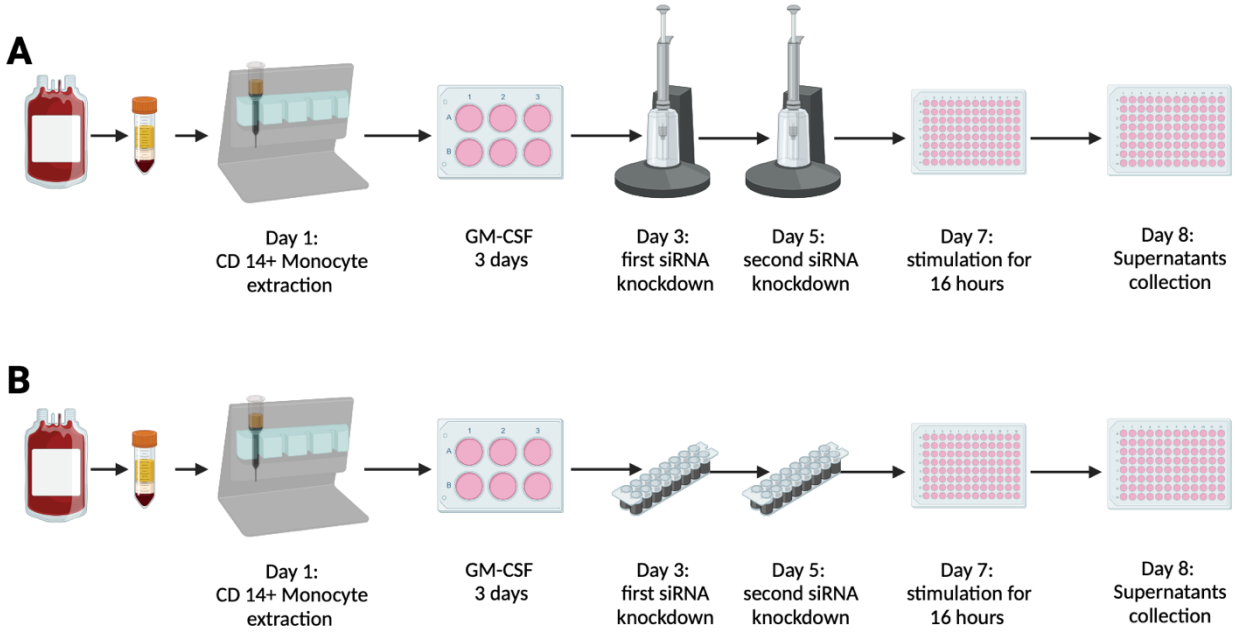

Figure 2: Schematic protocol of the knockdown experiment procedure.

This protocol applies for both siRNA-mediated knockdown techniques from **(A)** Invitrogen and **(B)** Lonza. The figure was created with biorender.com.

2.2.3.1 siRNA-mediated HDAC knockdowns with Invitrogen system

After 3 days of differentiation, the cells were harvested and counted. A total of 7 x 10^6 cells were used for each condition. Electroporation experiments were performed using the Neon Transfection System (MPK5000, Invitrogen) with 1.2 x 10^6 cells, 10 µl buffer T and 75 pmol (1.5 µl) siRNA per reaction. After electroporating the primary human macrophages in a 10 µl Neon Pipette Tip with the following electroporation conditions: 1400 V, 20 ms and 2 pulses, they were seeded into a 6-well plate containing 4 ml antibiotic-free 10 % FCS RPMI and 3.1 µl/ml GM-CSF. The electroporation was repeated

3 days after the first electroporation according to the protocol above, ensuring a high knockdown efficacy.

2.2.3.2 siRNA-mediated HDAC knockdowns with LONZA system

After extraction and differentiation of hMDM as described above, cells were harvested, washed twice in 10 ml PBS and counted. A total of 7 x 10^6 cells were used for each condition. The electroporation experiments were performed using the 4D Nucleofector core unit (LONZA) with 1 x 10^6 cells, 20 µl P3 nucleofection buffer and 0.75 µl of siRNA per reaction. Firstly, siRNA was added to the Lonza cassette strip. Subsequently, 20 µl of the cell/P3 nucleofection solution was added to the corresponding wells and cells were electroporated according to the pulse code: CM-137. Immediately after electroporation, 120 µl of antibiotic-free 10 % FCS RPMI was added to each cassette well. Cells were cultured in complete RPMI and 3.1µl/ml GM-CSF in 2 x 10^6 cells in 5 ml in a 6-well plate at 37°C, 5 % CO_2.
Knockdown efficacy was checked one day after the siRNA-mediated knockdown by WES as described below. Electroporation was repeated after two days according to above protocol to ensure a high knockdown efficacy.

2.2.4 Stimulation of primary human monocyte derived macrophages

Three days after the second electroporation, primary human macrophages were stimulated under different conditions. For this, 1 x 10^5 of the electroporated cells were seeded in 96- well plates and 50 µl of stimuli were added to incubate for 16 hours. (LPS working concentration 1 ng/µl; butyrate working concentration 10 mM). Cell-free supernatants were then collected to perform homogenous time resolved fluorescence (HTFR).

2.2.5 HDAC inhibitor experiments in primary human macrophages

After extraction and differentiation of hMDM as described above, cells were seeded in a 96-well plate at a concentration of 0.1 x 10^6 cells in 100 µl complete RPMI containing 3.1µl/ml GM-CSF. 50 µl of the HDAC inhibitors were incubated for 20 minutes prior to the addition of either 50 µl of LPS or complete RPMI (working concentrations are indicated in

Table 8). After 16 hours of cell stimulation, the supernatants were collected and cytokine levels were quantified by HTRF. In addition, cell lysates were collected to perform WES for protein detection and qPCR for gene expression analysis.

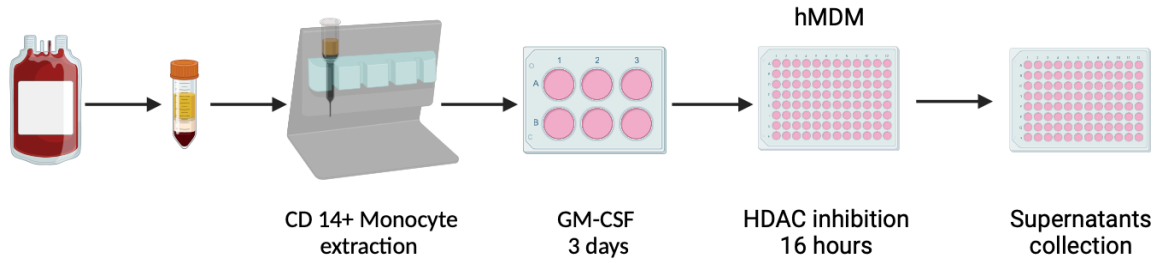

Figure 3: Schematic protocol of HDAC inhibitor experiments.
After extracting monocytes from buffy coats, cells were differentiated for 3 days in the presence of GM-CSF into macrophages. Then, HDAC enzymes were inhibited for 16 hours and supernatants and cell lysates were collected for further experiments. This figure was created with biorender.com.

Table 8: List of HDAC inhibitors and working concentrations

HDAC inhibitor	**Working concentration**
Abexinostat (PCI 24781)	100 nM
CUDC 101	20 nM
Fimepinostat (CUDC-907)	100 nM
LMK 235	20 nM
Mocetinostat (MGCD 0103)	2 µM
Panobinostat	1 µM
Quisinostat (JNJ 26481585)	5 mM
SIS-17	1 µM
SR-4370	4 µM
TMP-195	300 nM
TSA	0.5 µM
Tubacin	50 nM
Vorinostat (SAHA)	1 µM

2.2.6 Homogenous Time Resolved Fluorescence

Quantification of human cytokines was performed by homogenous time resolved fluorescence (HTRF) (Cisbio) according to the manufacturer's protocol. In brief, to measure cytokine levels, 3 µl of a prepared antibody mixture containing donor and acceptor antibodies in a 1:1 ratio was transferred to a 384-well HTRF plate (white) and was mixed with 12 µl of the cell-free supernatants collected from the stimulated hMDMs. For measurement of TNF-α cytokine levels, the cell-free supernatant was diluted 1:3 with complete RPMI. Plates were sealed with foil, centrifuged and incubated for 3 hours at room temperature. Fluorescence of donor and acceptor antibodies was measured at 620 nm and 688 nm using the SpectraMax i3 system.

2.2.7 mRNA expression level analysis

2.2.7.1 RNA isolation

After stimulation of 2.0 x 10^6 hMDMs per well for 16 hours in a 12-well plate, cells were washed twice with cold PBS and then lysed in 350 µl RLT lysis buffer (Qiagen) containing 1 % (v/v) β-mercaptoethanol. Cell lysates were transferred to new Eppendorf tubes and RNA was extracted according to the Qiagen RNeasy® Mini Kit Qick Start Protocol including on-column DNase digestion. Finally, RNA was eluted with 30 µl nuclease free water and checked for concentration and quality using NanoDrop™ one spectrophotometer.

2.2.7.2 cDNA synthesis

In this project, reverse transcription-polymerase chain reaction (RT-PCR) was used to synthesize cDNA from 200 ng- 800 ng of RNA from each sample. The RNA concentrations were adjusted for each sample by dilution with RNase-free water to 12.9 µl. Then, 1 µl of the oligo-dT primer was added to each sample and the samples were heated at 65°C for 5 minutes. After incubation for 1 minute on ice, 6.1 µl of a master mix containing 4 µl 5 x reaction buffer, 1 µl 0.1M DTT, 1 µl 10 mM dNTPs and 0.1 µl Superscript III reverse transcriptase was added to each tube. To check the efficiency of reverse transcription, a negative control without reverse transcriptase enzyme (- RT sample) was included. cDNA

was generated by incubating the samples for 50 minutes at 50°C followed by 5 minutes at 85°C.

2.2.7.3 Quantitative real-time PCR

In order to quantify gene expression by measuring the level of mRNA, a quantitative real-time PCR (qPCR) reaction was performed. The cDNA was diluted 1:5 with nuclease free water. In addition, a primer stock containing forward primer (2 µM) and reverse primer (2 µM) was prepared. Then, 8 µl qPCR master mix containing 2 µl primer stock, 5 µl SYBR green and 1 µl nuclease free water was pipetted into a 384-well qPCR plate and 2 µl of the diluted cDNA was added. After the plate was sealed with an adhesive film and briefly centrifuged, qPCR was performed on a QuantStudio 6 Flex real-time PCR system based on the settings indicated in Table 9. The data of mRNA expression levels were analyzed according to the $2^{-\Delta\Delta Ct}$ method and normalized to the housekeeping gene HPRT.

Table 9: Thermal cycler settings for qPCR experiments

Stage	**Hold**	**PCR**		**Melt Curve**		
Step	1	1	2	1	2	3
Temperature (in °C)	95	95	60	95	60	95
Time (in minutes)	1:00	0:01	0:20	0:15	1:00	1:00
Cycle number	-	40		-		

2.2.8 Western blot and Simple Western assay on WES™

To detect and analyze the protein expression from cell lysates Western blot and Simple Western assay on WES™ (WES) were performed. For Wes 0.25 x 10^6 HDAC knockdown cells and HDACi treated cells were seeded in 500 µl complete RPMI in a 24-well plate. For Western analysis 2 x 10^6 GM-CSF treated hMDM were incubated either with medium alone, butyrate, LPS or a combination of both and were seeded in 500 µl complete RPMI in a 24-well plate.

2.2.8.1 Sample preparation

After checking the cells adherence, the supernatants were removed and the cells were washed twice with 500 µl cold PBS. Subsequently, 35 µl of fresh RIPA lysis buffer was added, the cells were scraped, and the cell lysates were transferred to 1.5 ml Eppendorf tubes. Next, lysates were cleared of DNA by centrifugation for 10 minutes, 19,000 g at 4°C. Finally, the supernatant containing the protein lysate was transferred to a new 1.5 ml Eppendorf tube and was further used for protein quantification and WES.

2.2.8.2 Protein quantification

To ensure equal protein levels for WES, protein concentrations were quantified using the bicinchoninic acid (BCA) assay. In brief, protein lysates were diluted 1:5 using ddH_2O and transferred to a 96-well U-bottom plate. A standard serial dilution of BSA was prepared according to the manufacturer's protocol. Next, 200 µl of BCA Pierce reagent (1 x Reagent A, 50 x Reagent B) was added to all samples and standards. After 30 minutes of incubation at 37°C, the protein concentration was measured at 562 nm using the SpectraMax i3 system.

2.2.8.3 Simple Western assay

Most of the protein lysates were analyzed using the WES™ protein detection system by Simple Western. To perform WES, 4 parts of the cell lysates were mixed with 1 part of the 5x fluorescent master mix (supplied in protein simple kit) in PCR tubes. After heating the ladder and samples at 95°C for 5 minutes, they were loaded onto the separation microplate pre-filled with Split Running Buffer, Wash Buffer and 10 x Sample Buffer according to the manufacturer’s protocol. Next, the separation plate was centrifuged for 5 minutes at 800 x g. The samples were electrophoretically separated by a 25-capillary cartridge (12-230 kDa) with the settings stated in Table 10.

Table 10: Settings WES

Steps	**Duration**
Loading time of the separation matrix	200 s
Loading time of the stacking matrix	15 s
Loading time of the samples	9 s
Separation time of the samples at 375 V	25 min
Incubation time with the antibody diluent	5 min
Incubation time with the primary antibody	90 min
Incubation time with the secondary antibody	30 min

The results were processed and analyzed with the Compass for Simple Western software.

2.2.8.4 SDS-PAGE

For protein expression analysis by means of Western blot, 2 x 10^6 cells were seeded in 6-well cell culture plates and stimulated for 16 hours. For the subsequent preparation of cell lysates, RIPA lysis buffer was prepared from a 2 x stock solution and supplemented with 0.1 µM PMSF and complete EDTA-free protease inhibitor cocktail. While working on ice, supernatants were removed, cells were washed twice with ice-cold PBS and lysed with complete RIPA buffer. Following 15 minutes incubation on ice, cells were scraped off and transferred into 1.5 ml centrifuge tubes, followed by a two-pulse sonication.
For reducing gel electrophoresis, cell lysates were mixed with 4 x LDS sample buffer supplemented with 10 x sample reducing agent and were heated at 85°C for 10 minutes. Equal amounts of proteins were loaded on pre-cast 4-12 % Bis-Tris gels and separated by gel electrophoresis in MOPS or MES running buffer at 150 V for 1 hour. PageRuler™ Plus Prestained protein ladder ranging from 10 to 250 kDa was used as a size standard.

2.2.8.5 Western blot

Subsequently, proteins were transferred to a methanol-activated PVDF membrane using a semi-wet transfer unit at 32 V for 1.5 hours. Membrane blocking was performed for 1 hour in blocking buffer. Then, Primary antibodies were diluted in 1 % BSA in TBS-T and

incubated overnight at 4°C. Following three washes in TBS-T, the membranes were incubated with the respective IRDye secondary antibody diluted in 1 % BSA in TBS-T for 1 hour in the dark. Finally, the membranes were washed twice in TBS-T and once in 1 x TBS and the infrared fluorescent signals on the membranes were visualized using the Odyssey imager.

2.2.9 Chromatin Immunoprecipitation sequencing (ChIP-seq)

Samples for ChIP-Sequencing were generated and snap-frozen at the Institute of Innate Immunity (Bonn, Germany), while ChIP-Sequencing and analysis was performed in collaboration with Sergi Cuartero (Josep Carreras Leukaemia Research Institute, Barcelona, Spain).

For chromatin immunoprecipitation sequencing, 10 x 10^6 GM-MDMs were incubated with butyrate both in the presence and absence of LPS for 16 hours. Subsequently, cells were cross-linked with 1 % formaldehyde, lysed and sonicated in a mixture of 1 % Triton, 0.1 % sodium deoxycholate, 0.5 % SDS, 0.2 M NaCl, 10 mM Tris, pH 7.5, 10 mM EDTA and 1 x protease inhibitor cocktail. The samples were sonicated using a Covaris M220 focused ultrasonicator with the following setting: 75 % peak incident power (PIP), 200 cycles per burst (CPB), at 7ºC and 10 % DF for 15 minutes in lysis buffer containing 0.5 % SDS. The lysates, incubated overnight at 4ºC with 4 µg of H3K27ac antibody, were supplemented with 50 ng of *Drosophila* spike-in chromatin and 2 µg of spike-in antibody for normalization. Next, protein G Dynabeads were used to pull down antibody-bound chromatin. After samples were washed, RNase-treated and reverse cross-linked by incubation at 65°C in 1 % SDS, 0.1 M $NaHCO_3$ and proteinase K, ChIP DNA Clean & Concentrator Kit was used to purify the DNA. The NEBNext Ultra DNA Library Prep kit was utilized for library preparation.

2.2.9.1 ChIP-seq data processing

ChIP-seq libraries and input libraries were sequenced as paired-end 150 bp reads. Then, reads underwent alignment to the mouse genome mm39 and fruit fly genome dm6 through Bowtie 2 version 2.4.4, using '—very-sensitive' flag and a minimum fragment length (-X

flag) of 1000 bp, with default settings for the other parameter. The spike-in chromatin-based normalization was conducted within each biological replicate, scaling factors were calculated per sample as the ratio of total uniquely aligned counts to Drosophila compared to the counts in the sample with the least number of Drosophila counts and reads were down-sampled accordingly. Quality assessment of ChIP-Seq libraries was performed using ChIPQC. In fact, duplicate reads were identified and removed using Picard MarkDuplicates. Next, the genome-wide coverage tracks in bigwig format were generated via DeepTools' bam Coverage (v. 3.3.1). MACS2 (v. 2.2.5) was employed to identify ChIP-Seq Peaks, utilizing input libraries as control. The average ChIP-seq signal around transcription start sides (TSS) and intergenic peaks (>5 kb from the closest gene) were computed and graphed using deep Tools with bigwig files as input (v. 3.3.1, compute Matrix and plotProfile, respectively). For the quantification of H3K27ac signal at promoters, ChIP-seq reads were quantified at promoters (+ - 500 bp of transcription start site) of all genes previously analyzed by RNA-seq. Differential ChIP-signal between samples was analyzed using DESeq2, avoiding default normalization as ChIP-seq signal had already been normalized by spike-in chromatin.

2.2.10 Statistical Analysis

Data - and statistical analysis were performed with GraphPad Prism version 10. After checking for normal distribution, two-way analysis of variances (ANOVA) was applied with multiple comparison correction according to Šídák and Tukey. Data is presented as mean + standard error of the mean (SEM). A p-value of maximally 0.05 was considered as statistically significant. The significance was visualized in the graphs with: * = $p < 0.05$, ** = $p < 0.01$, *** = $p < 0.001$, **** = $p < 0.0001$

3 Results

In order to investigate the effect of HDAC inhibition by the SCFA butyrate on the TLR-4-induced IL-10 signaling, rhGM-CSF-differentiated primary human MDMs (GM-MDMs) were exposed to LPS both with and without butyrate for 16 hours, mimicking the leaky gut macrophage microenvironment during inflammation *in vitro*.

3.1 The impact of single HDAC knockdown in primary human macrophages

Initially, the impact of a single HDAC knockdown on IL-10 cytokine levels after 16 hours of LPS treatment in both the presence and absence of the SCFA butyrate was assessed. Knockdown efficacy was evaluated by two siRNA-mediated interventions in GM-MDMs using WES, as shown in Figure 4.

Scrambled siRNA was used as control. The siRNA-induced knockdown showed an effective reduction of HDAC 1, HDAC 4, HDAC 6, HDAC 7, and HDAC 8 expression, while knockdown of HDAC 9 was less efficient. HDAC3 showed only minimal expression levels in GM-MDMs.

Upon evaluation of IL-10 cytokine levels following two siRNA-mediated knockdowns and 16 hours of LPS exposure in the supernatants of primary human rhGM-CSF macrophages, no difference was observed between the knockdown sample and the control (Figure 5 A). Interestingly, after HDAC 8 knockdown and LPS treatment, IL-10 levels increased compared to the control (Figure 5 A). Medium alone did not induce IL-10 production. This was also observed when GM-MDMs were incubated together with LPS and butyrate, indicating that butyrate suppresses the LPS-induced IL-10 production (Figure 5 A).

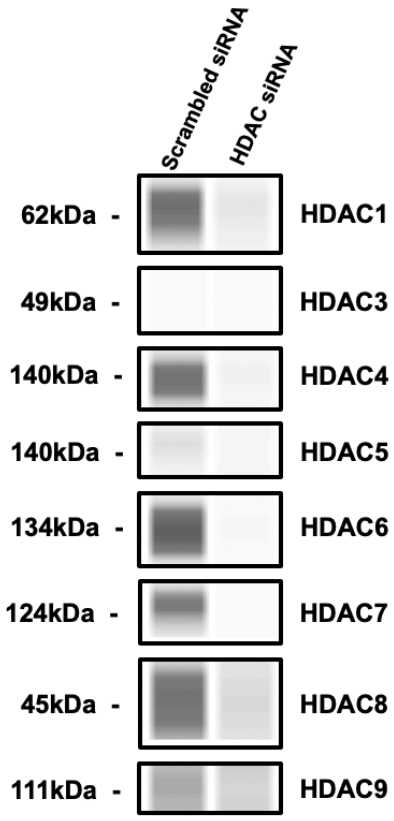

Figure 4: Knockdown efficiency in primary human GM-CSF macrophages.
The knockdown efficiency after two runs of siRNA mediated knockdown experiments with the Invitrogen system indicated for HDAC 1, 3, 4, 5, 6, 7, 8 and 9, for control siRNA and indicated knockdown. Figure (adapted) from Wang et al., 2024.

IL-6 cytokine levels did not differ between HDAC knockdown and control (Figure 5 B). Moreover, the administration of LPS in combination with butyrate had no blocking effect on the IL-6 secretion (Figure 5 B). GM-MDMs showed an appropriate inflammatory response to the LPS stimulus by secreting TNF-α (Figure 5 C). These levels did not differ between the knocked down samples and the control. Furthermore, medium alone did not induce TNF-α secretion (Figure 5 C).

Taken together, these results indicate that the SCFA butyrate suppresses the TLR4-mediated IL-10 secretion and that this mechanism is not attributed to a single HDAC inhibition but rather implies the involvement of a group of HDACs.

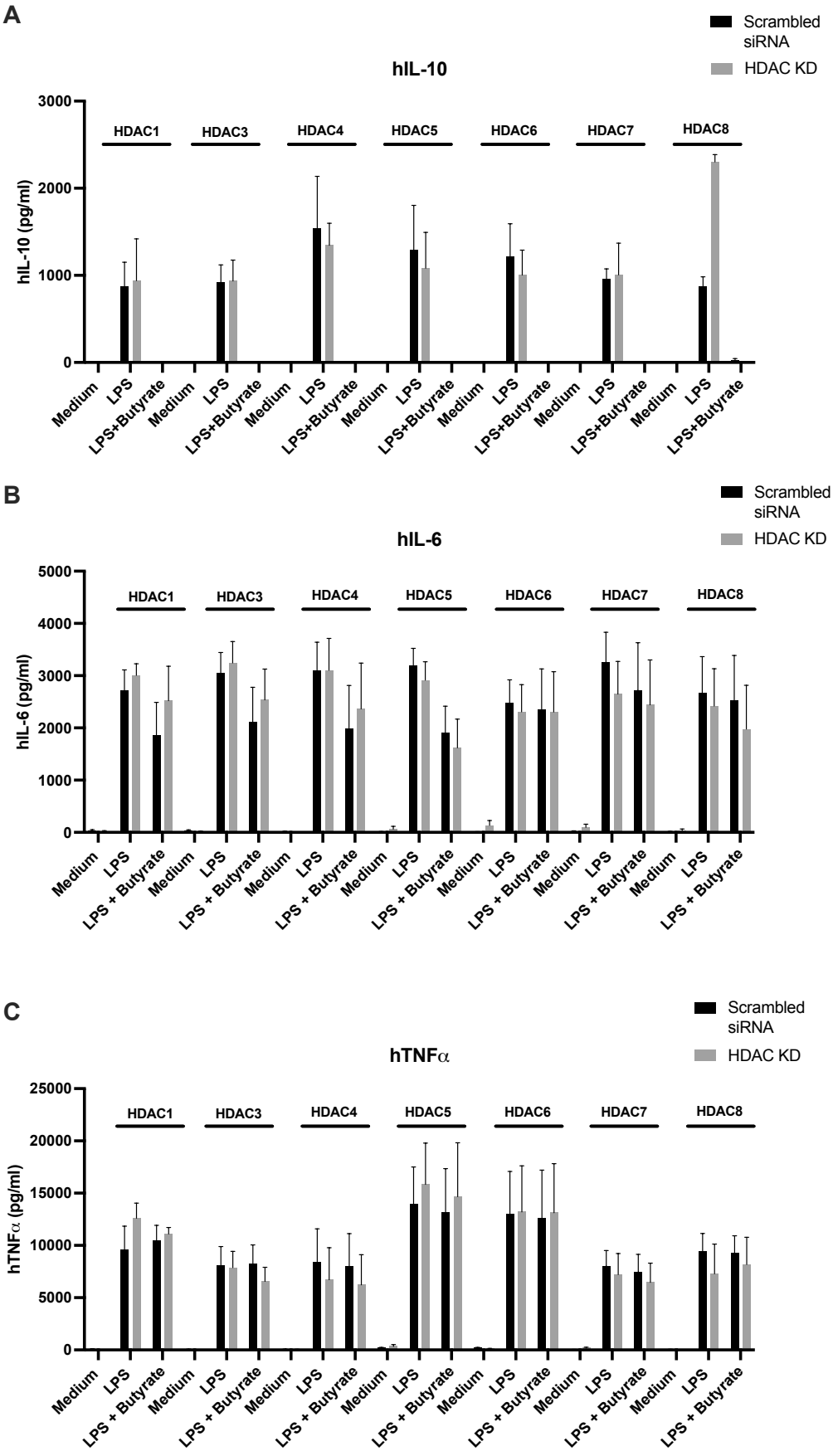
A
Scrambled siRNA
HDAC KD
hIL-10
hIL-10 (pg/ml)
3000
2000
1000
0
HDAC1
HDAC3
HDAC4
HDAC5
HDAC6
HDAC7
HDAC8
Medium
LPS
LPS+Butyrate
B
Scrambled siRNA
HDAC KD
hIL-6
hIL-6 (pg/ml)
5000
4000
3000
2000
1000
0
HDAC1
HDAC3
HDAC4
HDAC5
HDAC6
HDAC7
HDAC8
Medium
LPS
LPS + Butyrate
C
Scrambled siRNA
HDAC KD
hTNFα
hTNFα (pg/ml)
25000
20000
15000
10000
5000
0
HDAC1
HDAC3
HDAC4
HDAC5
HDAC6
HDAC7
HDAC8
Medium
LPS
LPS + Butyrate

Figure 5: **Effect of single HDAC knockdown on IL-10 secretion.**
(A-C): GM-MDMs were electroporated with siRNA either targeting HDAC1, HDAC3, HDAC4, HDAC5, HDAC6, HDAC7, HDAC8 or scrambled siRNA before stimulations with medium, LPS (1 ng/ml) and LPS (1 ng/ml) + butyrate (10 mM) for 16 hours. The levels of **(A)** IL-10, **(B)** (IL-6) and **(C)** TNF-α in the cell-free supernatants were measured by HTRF. Pooled data from n = 4 (HDAC 1-7) and n = 2 (HDAC 8), each in technical duplicate, mean + SEM. n.s. by Two-way ANOVA with Tukey's multiple comparison test. HDAC KD = HDAC knockdown. Figure (adapted) from Wang et al., 2024.

3.2 The impact of HDAC inhibitors on IL-10 levels in primary human macrophages

Next, HDAC inhibitors with varying specificities were employed to evaluate their potential to recapitulate the effects of the SCFA butyrate on LPS-induced IL-10 signaling (Figure 6 A).

First of all, the HDAC inhibitory capacity of the applied compounds was assessed by checking their ability to increase the acetylation lysine 27 residue of histone 3 (H3K27) in the presence of LPS in GM-CSF macrophages after 16 hours. LPS treatment alone did not change the acetylation level of H3K27 (Figure 6 B). However, an incubation of GM-CSF macrophages with the HDACis Panobinostat, Vorinostat, Abexinostat, Fimepinostat, Quisinostat and SR4370 significantly increased H3K27 acetylation (Figure 6 B). TMP 195, LMK 235, SIS-17 and Tubacin did not change the acetylation level of H3K27 (Figure 6 B). Remarkably, TSA which is considered as a pan-HDAC inhibitor was also not able to change H3K27 acetylation (Figure 6 B).

Subsequently, GM-CSF macrophages were incubated with HDAC inhibitors and butyrate both in the presence and absence of LPS for 16 hours, followed by cytokine detection by HTRF. Panobinostat, Vorinostat, and TSA, all classified as pan-HDAC inhibitors, completely suppressed IL-10 secretion after 16 hours of incubation with LPS, similar to butyrate (Figure 6 C). Notably, comparable results were observed with more selective HDACi targeting especially class I HDACs (HDACs 1-3 + 8) and HDAC 10 (Figure 6 C). These HDACi successfully mimicked the effect of butyrate in hMDM *in vitro*. However, HDACi targeting class IIa HDACs (HDAC 4, 5, 7, 9), class IV HDAC (HDAC 11) and HDAC 6 had no inhibitory effect on the LPS triggered IL-10 secretion (Figure 6 C).

Interestingly, HDACi that inhibited the LPS-induced IL-10 response triggered the release of IL-1β (Figure 6 E). Vorinostat and Quisinostat were, in addition to butyrate, both able to significantly elevate IL-1β levels following LPS stimulation (Figure 6 E). TMP, LMK, Tub and SIS that all induced IL-10 secretion, had no secreting effect on IL-1β (Figure 6 C, E). TNF-α and IL-6 cytokine levels were not affected by the treatment of HDACi (Figure 6 D, F).

Taken together, these results suggest, that the SCFA butyrate and the tested HDACi share a similar mechanism in suppressing IL-10 secretion induced by LPS in hMDMs, implicating HDACs 1-3, 8 and 10 as potentially crucial targets for this response. The HDAC inhibitors that were able to increase H3K27 acetylation were able to inhibit the LPS induced IL-10 secretion. Moreover, there might be a differential control between the cytokines IL-10 and IL-1β, since they are regulated in opposite directions.

A

HDAC Inhibitor	Targets
Panobinostat (Pan)	1-11
Vorinostat (Vor)	1-11
Trichostatin A (TSA)	1-11
Fimepinostat (Fim)	1-3, 6, 10, 11
Quisinostat (Quis)	1-5, 8, 10, 11
Mocetinostat (Moc)	1-3, 11
SR-4370 (SR)	1-3, 6, 8
Abexinostat (Abex)	1-3, 6, 8, 10
CUDC-101 (CUDC)	1-10
TMP-195 (TMP)	4, 5, 7, 9
LMK 235 (LMK)	4, 5
Tubacin (Tub)	6
SIS-17 (SIS)	11

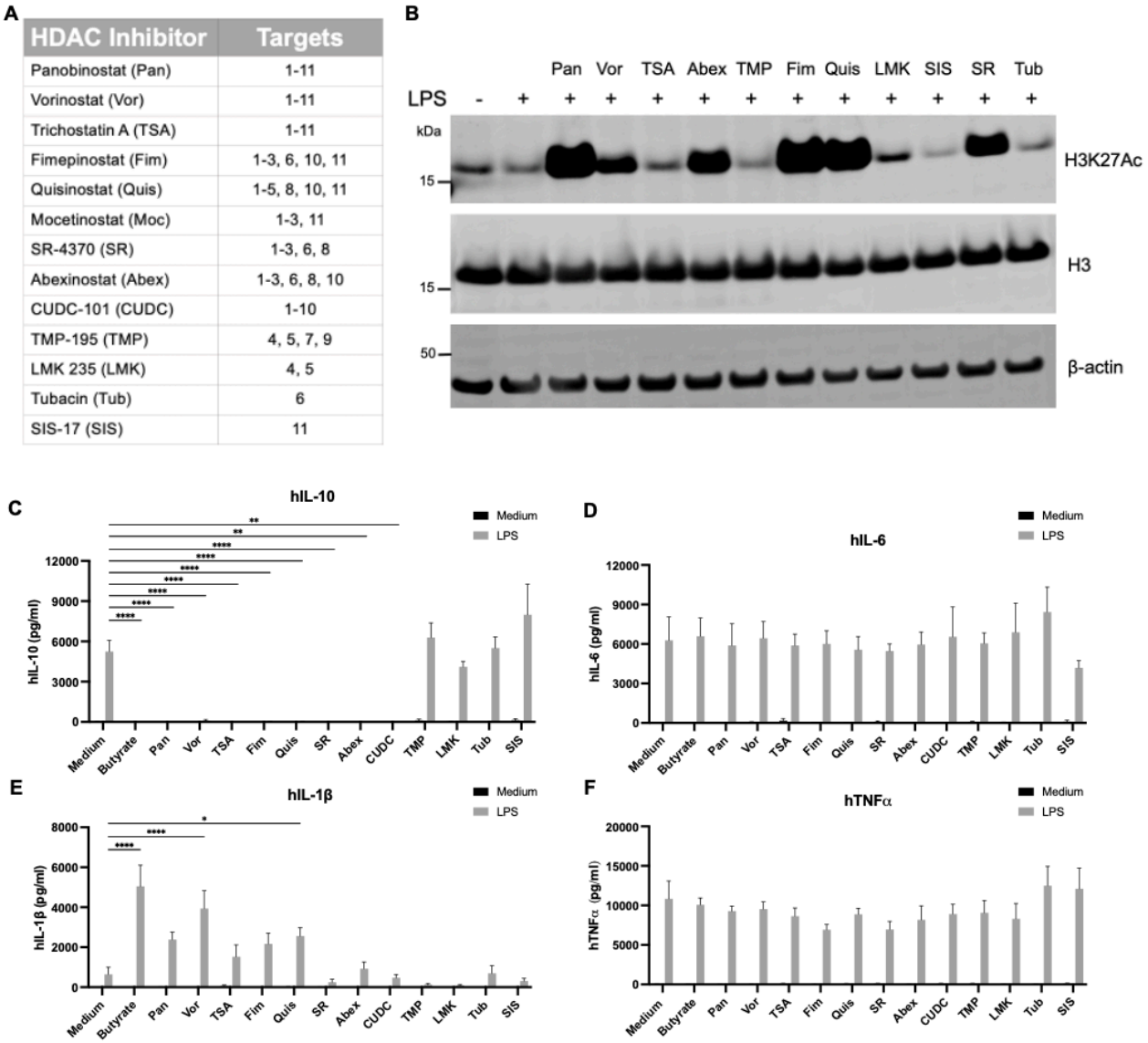

Figure 6: Effect of HDAC inhibitors on histone acetylation and cytokine levels. **(A)** HDAC inhibitors and their target specificities. **(B)** GM-MDMs were incubated with LPS alone or both LPS and the indicated HDAC inhibitor, for 16 hours. Levels of histone 3 K27 acetylated (H3K27ac), total histone 3 or β-actin were evaluated by western analysis. Blot is representative of three independent experiments. **(C-F):** GM-MDMs were treated with Butyrate (10 mM), Panobinostat (Pan) (1 μM), Vorinostat (Vor) (1 μM), TSA (0.5 μM), Fimepinostat (Fim) (0.1 μM), Quisinostat (Quis) (5 mM), SR4370 (SR) (4 μM), Abexinostat (Abex) (0.1 μM), CUDC-101 (CUDC) (0.02 μM), TMP195 (TMP) (0.3 μM), LMK235 (LMK) (0.02 μM), Tubacin (Tub) (0.05 μM), SIS-17 (SIS) (1 μM) alone or in combination with LPS for 16 hours. Cytokine levels of **(C)** IL-10, **(D)** IL-6, **(E)** IL-1β and **(F)** TNF-α in cell-free supernatants were assessed by HTRF. (B-E) Pooled data from n=5, each in technical duplicate, error bar represents mean + SEM, *p<0.05, **p<0.01, ***p<0.001, ****p<0.0001

by Two-way ANOVA with Šídák's multiple comparison test. Figure (adapted) from Wang et al., 2024.

3.3 Butyrate blocks IL-10 expression on transcriptional level in primary human macrophages

Subsequently, the impact of the SCFA butyrate and HDACi on the gene expression of IL-10, IL-1β, IL-6 and TNF-α was investigated. For this, hMDM were incubated with butyrate or any other HDACi in the presence or absence of LPS and mRNA expression levels were evaluated by relative qPCR (Figure 7).

IL-10 expression increased upon LPS stimulation (Figure 7 A). This LPS-induced IL-10 expression was completely blocked by butyrate and HDACi targeting class I HDACs and HDAC 10, suggesting a direct impact on mRNA expression by the tested compounds (Figure 7 A). SIS-17, which is a potent HDAC 11 inhibitor, failed to block the LPS mediated IL-10 release, increasing IL-10 gene expression approximately 40 times.

In contrast, HDAC inhibition had contrary effects on IL-1β mRNA expression. In the presence of LPS, butyrate and the HDAC inhibitors induced the transcription of IL-1β (Figure 7 B). This effect was seen for each HDAC inhibitor as well as butyrate used in this experiment

The TLR4-Agonist LPS was able to increase the mRNA expression of IL-6 and TNF-α in each condition. IL-6 gene expression fluctuates between the different HDAC inhibitors, however, in each sample an LPS-mediated increase of IL-6 transcription has been observed. Under non-stimulated conditions, baseline TNF-α transcription is present in each sample. Upon LPS stimulation, TNF-α transcription tends to rise minimally.

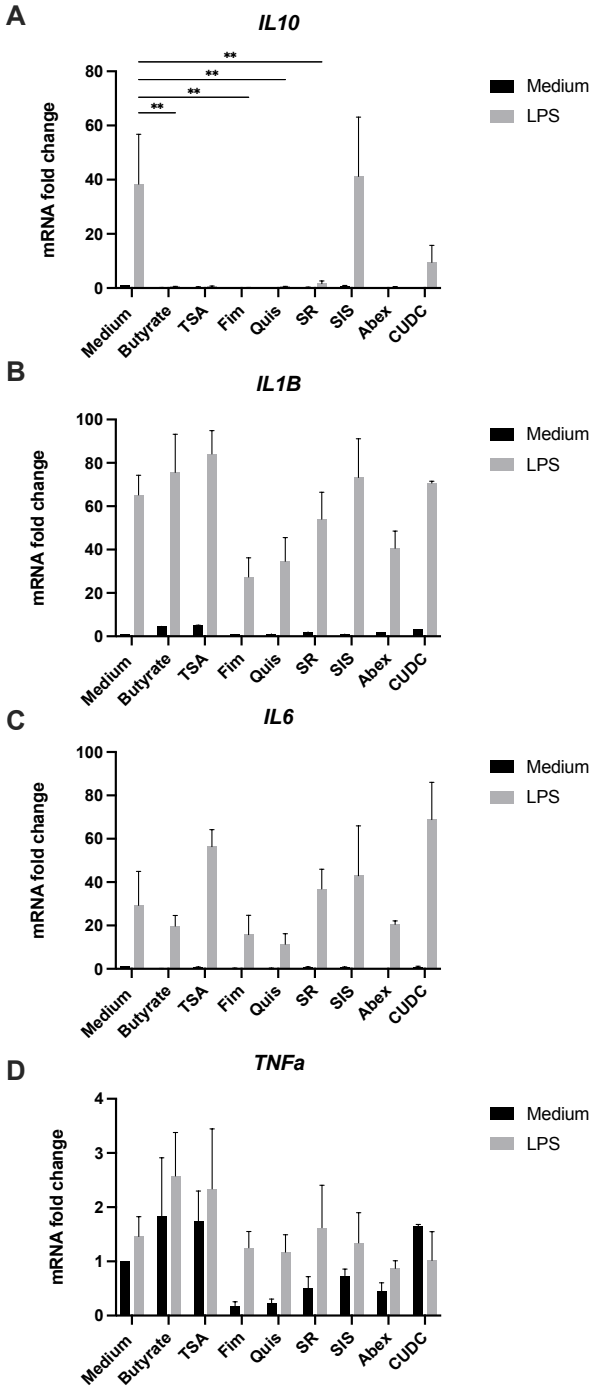

Figure 7: Butyrate blocks IL-10 expression on the transcriptional level.
(A-D): GM-MDMs were treated with Butyrate (10 mM), TSA (0.5 µM), Fimepinostat (Fim) (0.1 µM), Quisinostat (Quis) (5 µM), SR-43790 (SR) (4 µM), SIS-17 (SIS) (1 µM), Abexinostat (Abex) (0.1 µM), CUDC101 (0.02 µM) alone or in combination with LPS for 16 hours. mRNA levels were assessed for **(A)** IL-10, **(B)** IL-1β, **(C)** IL-6 and **(D)** TNF-α by qPCR. Pooled data from n=5 for Medium, Butyrate, Fim, Quis, SR, SIS, n=2 for TSA, Abex and CUDC, each in technical duplicate, error bars represent mean + SEM.
*p<0.05, **p<0.01, ***p<0.001, ****p<0.0001 by Two-way ANOVA with Šídák's multiple comparison test.

3.4 Impact of HDAC1-3 knockdown on LPS-induced IL-10 signaling in primary human macrophages

Since there was no effect of siRNA-mediated knockdown on individual HDACs and based on the data from the HDAC inhibitor experiments suggesting that class I HDACs are predominantly inhibited by butyrate, the next experiment was to downregulate class I HDACs excluding HDAC 8 due to the knockdown inefficacy.

To determine whether the TLR4-dependent IL-10 suppression by butyrate involves HDAC 1-3 inhibition, siRNA-mediated knockdowns of HDAC 1-3 were performed in hMDMs. Cytokine levels of IL-10 and TNF-α were assessed by HTRF and compared to the scrambled siRNA, both in the presence and absence of butyrate and LPS.

At first, the knockdown efficacy was assessed after two electroporation procedures for ensuring a high knockdown efficiency. HDAC 1, HDAC 2 and HDAC 3 protein levels were completely ablated after two siRNA-mediated knockdowns (Figure 8 A). Electroporation with scrambled siRNA had no blocking effect on HDAC 1, HDAC 2 and HDAC 3.

Interestingly, the combinatory HDAC 1-3 knockdown lead to a decrease in IL-10 level when compared to the scramble control in the presence of LPS. Neither butyrate alone, nor the combination of butyrate and LPS resulted in IL-10 secretion after electroporation with scrambled and HDAC 1-3 siRNA (Figure 8 B).
The knockdown of HDAC 1-3 resulted in minor decreases in TNF-α secretion in hMDMs (Figure 8 C). Both butyrate and medium alone were not able to trigger TNFα secretion.

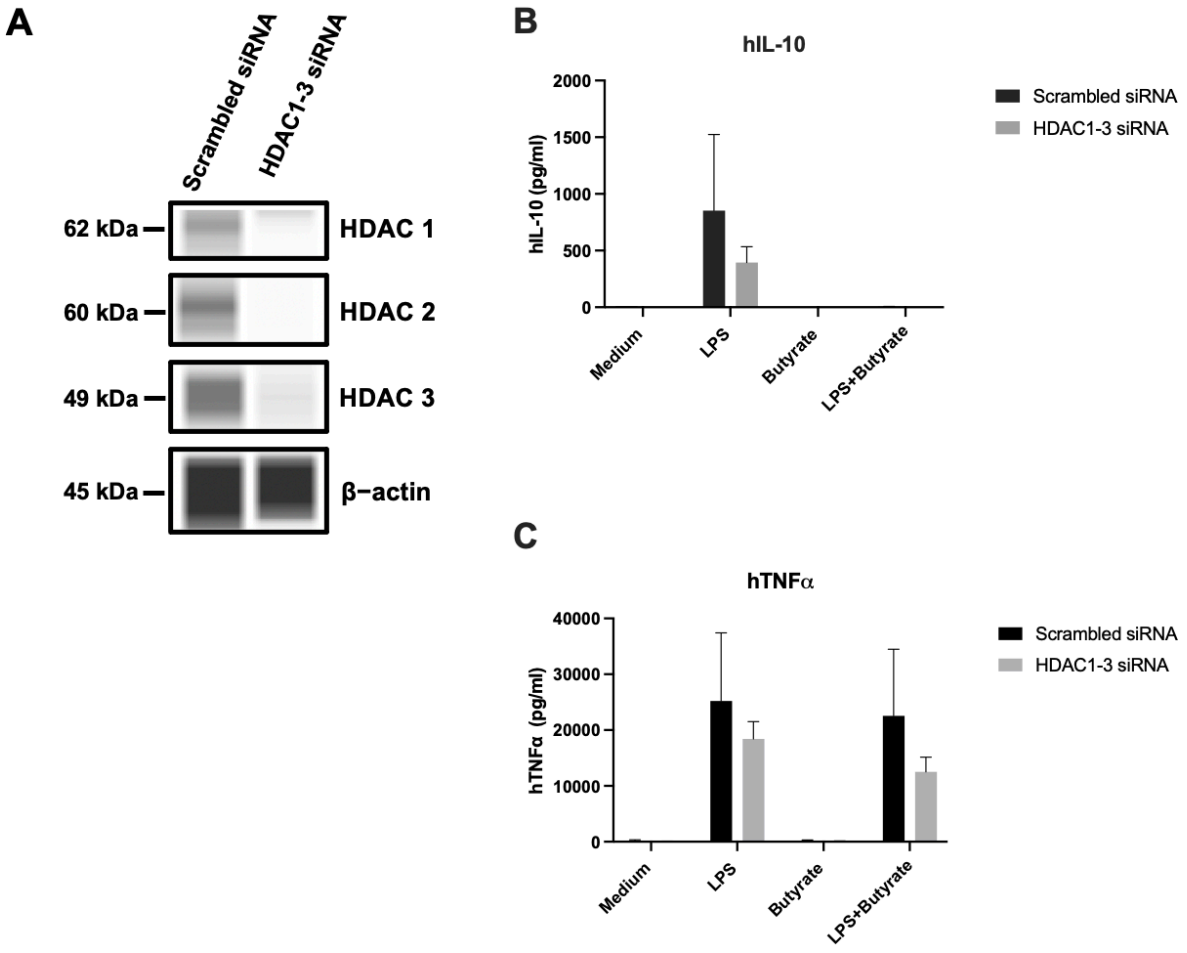

Figure 8: siRNA mediated HDAC1-3 knockdown.
(A) GM-MDMs were electroporated with either scrambled siRNA or a mix of HDAC1-3 siRNA. The knockdown efficiency of HDAC 1, HDAC 2 and HDAC 3 was evaluated by measuring the expression of HDAC 1, HDAC 2 and HDAC 3 after two electroporation procedures by WES; β-actin served as loading control. **(B-C)** GM-MDMs were electroporated with either scrambled siRNA or a mix of HDAC1-3 siRNA before the stimulations with medium, LPS (1 ng/ml) and LPS (1 ng/ml) + butyrate (10 mM) for 16 hours. The cytokine levels for **(B)** IL-10 and **(C)** TNF-α in the cell-free supernatants were measured by HTRF. Pooled data from n = 2 (B, C), each in technical duplicates, mean + SEM. (A) Blot is representative of two independent experiments.

3.5 Butyrate inhibits STAT3 phosphorylation via HDAC inhibition

To assess the impact of the SCFA butyrate and other HDACi on STAT3 activity, the phosphorylation status of STAT3 at the Tyr705 and Ser727 residues in human GM-MDMs in both TLR4-dependent and -independent context by means of WES was evaluated (Figure 9 A).

Interestingly, TLR4 agonist LPS induced the phosphorylation of STAT3 at both residues (Y705 and S727) which were completely inhibited by butyrate (Figure 9 A). Also, other PanHDACi were able to mimic this effect of butyrate with regard to Y705 phosphorylation of STAT3. However, when probing for S727 phosphorylation, the HDACi exerted their STAT3 regulatory function to a slightly lesser degree, compared to the effect exhibited by butyrate, but were still able to decrease phosphorylation of mitoSTAT3. The selective HDACi SIS-17 targeting HDAC 11 was not able to suppress the LPS-mediated STAT3 phosphorylation at Y705 nor at S727.

With respect to the cytokine levels, there is an LPS-mediated IL-10 suppression by butyrate, Fimepinostat, Quisinostat and Mocetinostat. Those compounds were also able to suppress the STAT3 phosphorylation of both residues (Figure 9 A, B). SIS-17, which was not able to inhibit pSTAT3, also did not suppress the IL-10 release in a TLR4 dependent manner. TNF-α cytokine levels increased in each condition after LPS stimulation (Figure 9 C).

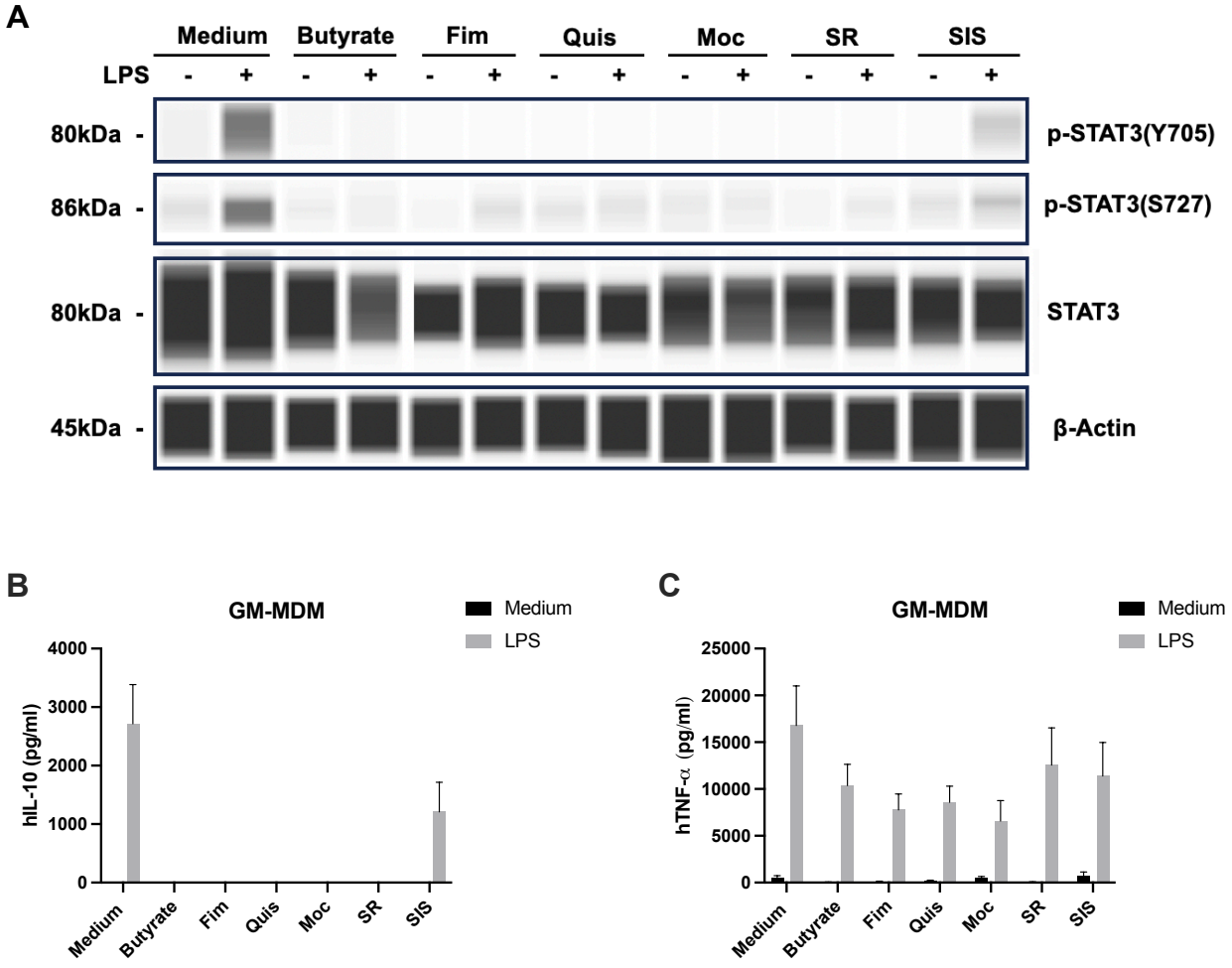

Figure 9: Butyrate inhibits STAT3 signaling via HDAC inhibition.
(A-C): GM-MDMs were treated with Butyrate (10 mM), TSA (0.5 µM), Fimepinostat (Fim) (0.1 µM), Quisinostat (Quis) (5 mM), Mocetinostat (Moc) (2 µM), SIS-17 (SIS) (1 µM), SR4370 (SR) (4 µM), alone or in combination with LPS (1ng/ml), for 16 hours. **(A)** Levels of phosphorylated STAT3 (Y705 + S727), total STAT3 and β-actin serving as loading control were evaluated by WES. **(B-C)** The cytokine levels of **(B)** IL-10 and **(C)** TNF-α in the cell free supernatants were measured by HTRF. Pooled data from n = 5 (B, C), each in technical duplicates, mean + SEM. (A) Blot is representative of 4 independent experiments.

3.6 Acetylation status of the *IL-10* gene locus

Since butyrate is a potent HDAC inhibitor, the influence of butyrate on the acetylation status of the histones in hMDM was investigated by Western blotting.

Butyrate administration resulted in an overall increase in histone 3 lysine 27 acetylation (H3K27ac) (Figure 10: H3K27 Acetylation status). This increase in H3K27ac was maintained after co-stimulation with LPS and butyrate. LPS alone had no effect on the acetylation of H3K27.

Next, the spread of enhanced H3K27ac across the genome using chromatin immunoprecipitation sequencing (ChIP-seq) was analyzed. The samples were normalized with spiked-in chromatin to adjust for the overall rise in acetylation levels upon co-stimulation with LPS and butyrate. The H3K27 at the IL-10 promoter revealed minimal increase in acetylation compared to other genes following butyrate and LPS treatment (Figure 10 B).

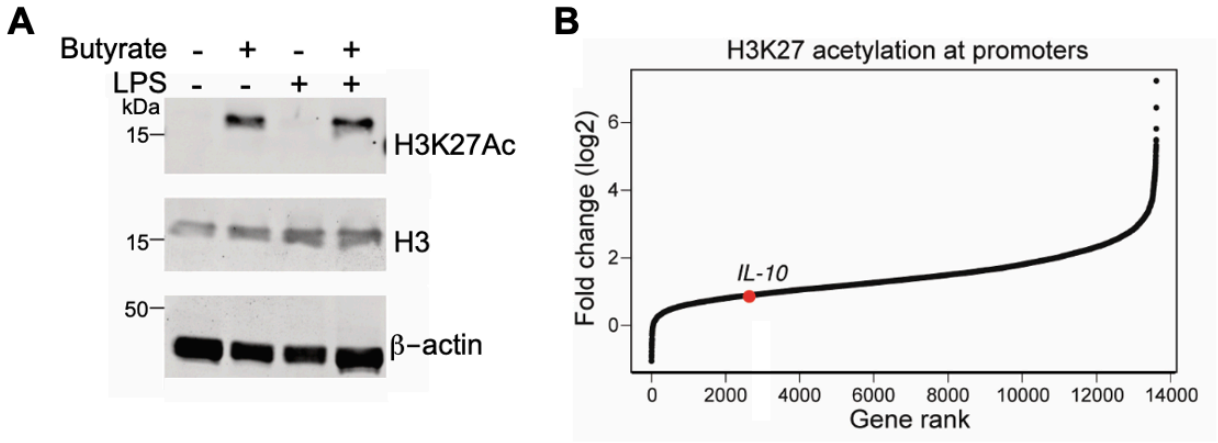

Figure 10: H3K27 Acetylation status.
(A) GM-MDMs were incubated with butyrate, LPS or a combination of both, for 8 hours. Levels of histone 3 K27 acetylated (H3K27ac), total histone 3 or β-actin were evaluated by western analysis. Blot is representative of three independent experiments.
(B) Total gene ranking ordered by the fold-change in H3K27 acetylation signals in LPS and butyrate treated samples indicating the IL-10 promoter. Figure (adapted) from Wang et al., 2024.

4 Discussion

Up to date, there is no specific curative treatment available for IBD. Extensive research has focused on investigating the influence of microbiome-derived metabolites, particularly SCFAs such as butyrate, on maintaining intestinal homeostasis by modulating the cross-talk between the microbiome and the immune system. Although butyrate is known for its potent anti-inflammatory properties under steady-state conditions, its application in acute inflammatory conditions within the GIT has presented contradictory outcomes, often exacerbating symptoms in patients. The impact of butyrate on the immune response under inflammatory conditions of the GIT associated with a permeable intestinal barrier remains to be explored. In this study, the influence of the SCFA butyrate on cytokines in GM-MDMs under inflammatory conditions was investigated with a special focus on the IL-10 regulation. In addition, HDAC inhibitory properties of butyrate during inflammation in GM-MDMs were examined to further understand its characteristics in the pathogenesis of IBD. In order to mimic the leaky gut microenvironment during inflammation, *in vitro* primary human macrophages were co-stimulated with LPS and butyrate or HDAC inhibitors.

4.1 Butyrate exerts pro-inflammatory effects on GM-CSF macrophages in a TLR4-dependent manner

Under steady-state conditions, butyrate administration leads to a reduction in the gene expression of macrophage pro-inflammatory mediators including nitric oxide (NO) and IL-12 which is attributed to the HDAC inhibition (Chang et al., 2014). In contrast to this antimicrobial response typically induced by SCFAs in macrophages under stable conditions, our results show that butyrate induces a pro-inflammatory program when macrophages are exposed to the PAMP LPS simultaneously. In this study, butyrate was shown to entirely inhibit the LPS induced anti-inflammatory and gut homeostasis-driving cytokine IL-10, both with regard to expression and secretion in hMDM. This is in line with previous studies reporting the suppressive effect of butyrate in combination with LPS on IL-10 levels in monocytes (Cox et al., 2009).

Strikingly, we were even able to demonstrate IL-1β secretion upon macrophage stimulation with butyrate and LPS. IL-1β is a strong pro-inflammatory cytokine, usually released by pyroptotic cells upon inflammasome activation (Latz et al., 2013). However,

further investigations on inflammasome induction mediated by butyrate were beyond the scope of this thesis. Of note, Park et al. recently reported NLRP3 inflammasome and caspase-1 activation, as well as IL-1β secretion in THP-1 cells upon treatment with *E. faecalis* and butyrate (Park et al., 2023). In contrast to that, butyrate was previously always described as an inhibitor of the NLRP3 inflammasome, in line with its well-appreciated anti-inflammatory and homeostatic function in physiology (Bian et al., 2017; Jiang et al., 2020; Yuan et al., 2018).

Other cytokines, such as TNF-α and IL-6 remained unaffected by butyrate. Based on these outcomes, the anti-inflammatory effect of butyrate is diminished under conditions of acute GIT inflammation, highlighting its context-dependent effects. This context specific effect has been described previously. In fact, IL-10 responsiveness was shown to depend on the environment of the inflamed tissue (Wilbers et al., 2018).

4.2 Pro-inflammatory effect of butyrate depends on HDAC Inhibition in GM-CSF macrophages

The SCFA butyrate is able to both signal via GPCR or by direct HDAC inhibition (Hodgkinson et al., 2023). Previously it was demonstrated that the antimicrobial activity of butyrate is independent of GPCR signaling, as macrophages co-cultured with butyrate and the GPCR inhibitor pertussis toxin still showed enhanced antibacterial activity (Chang et al., 2014; Schulthess et al., 2019). In line with that, I found in this study that butyrate acts via HDAC inhibition on the modulation of cytokine levels and gene expression in hMDMs, predominantly suppressing IL-10. Based on the experiments performed, the HDAC inhibitory compounds had similar effects on the cytokine profiles and gene expression of macrophages as butyrate, supporting the HDAC inhibitory function of butyrate. HDACs are enzymes, generally known for their ability to remove acetyl groups from lysine residues of histone proteins, allowing DNA to wrap more tightly around histones thereby regulating transcription (Milazzo et al., 2020). Following inhibition of HDAC enzymes by the SCFA butyrate, a global hyperacetylation results, altering chromatin structure thereby influencing gene expression. In support of this, an increase in H3K27 acetylation was observed after incubation of GM-CSF macrophages with butyrate in this study, suggesting that butyrate induces an accumulation of histone acetylation at

histone 3 lysine 27 via HDAC inhibition. Similarly, in bone marrow-derived macrophages, increased acetylation of histone 3 lysine 9 was observed by butyrate (Chang et al., 2014). Histone hyperacetylation is generally considered as marker for transcriptional activation. Interestingly, the ChIP-sequencing data revealed that although there was a genome-wide increase in H3K27ac, the *IL-10* promoter only showed a comparably low increase in acetylation. Nonetheless, IL10 expression was completely blunted after LPS and butyrate treatment. One explanation for this might be that HDAC inhibition induced by the SCFA butyrate results in a state of histone hyperacetylation, subsequently overloading the transcriptional machinery, being the limiting factor for transcription. Likewise, Chang et al. demonstrated a decrease in RNA polymerase II (pol II) and the serine 5-phosphorylated form of pol II (S5P), which are markers of transcriptional initiation, in the presence of butyrate at several response genes (Chang et al., 2014).

This study showed that cytokine and mRNA levels of IL-10 and IL-1β were differentially regulated following LPS and butyrate stimulation. While IL-10 secretion was completely blunted, an increase in IL-1β was observed, whereas this effect was not seen for other cytokines such as IL-6 and TNF-α.

One possible explanation for this observation lies in the epigenetic regulation of butyrate via its HDAC inhibitory capacity. As previously mentioned, we observed a genome-wide increase in H3K27ac following butyrate administration. Although being a global effect, some parts of the genome are less affected by butyrate's HDAC-inhibitory effect, as demonstrated for the IL-10 promoter, thereby potentially explaining the differential regulation of the studied cytokines. The state of histone hyperacetylation and the resulting overloading of the transcriptional machinery might therefore result in a loss of transcription at promoters that are less accessible. This epigenetic regulation might explain the differential expression of IL-10 being switched off, while other hyperacetylated promoters remaining unaffected from the overload of the transcriptional machinery such as IL-1β.

4.3 Butyrate acts pro-inflammatory via class I HDAC inhibition in GM-CSF macrophages

Since butyrate is able to inhibit HDACs and thereby exerts its LPS-dependent pro-inflammatory effects, it is important to know which HDACs exactly are inhibited by butyrate and thereby influence gene expression. In humans, HDAC enzymes are grouped into 4 classes: Class I HDACs (HDAC 1-3, 8), class II HDACs (HDAC 4-10), class III HDACs

(Sirtuins) and class IV HDACs (HDAC 11) (Yoon and Eom, 2016). The inhibitory function of butyrate on different HDACs was studied before in various contexts. For example, class I HDACi but not class II HDACi were able to mimic the butyrate effect on beta cell differentiation of neonatal porcine islet cells into beta cells (Zhang et al., 2021). In conjunction with this finding, in this study, the primary effect of butyrate of inhibiting the LPS-induced IL-10 release was mimicked by HDAC inhibitory compounds that target class I HDACs underlining the specific action of butyrate towards a pro-inflammatory environment in GM-CSF macrophages.

In contrast to our results, SAHA (Vorinostat), which is considered a pan-HDACi, was described earlier to improve intestinal inflammation in an IBD mouse model (Glauben et al., 2006). One explanation for the conflicting results might be the use of a different species. Our study focused on primary human cells in order to study butyrate-mediated cytokine responses, which is a closer model to human IBD than mice, since immune cell responses may highly vary in different species. However, the complex interplay between immune cells, bacteria, and intestinal epithelial cells that is prevalent in the GIT remains to be elucidated.

The ability of butyrate to epigenetically regulate the expression of IL-10 and IL-1β can be linked to its vita-PAMP activity. Vita-PAMPs are viability related PAMPs, that are present on or produced by living microbes and can be recognized by the immune system such as bacterial mRNA (Mourao-Sa et al., 2013). Butyrate is generated solely by living bacteria and is identified by macrophages as a sign of possible danger. Therefore, under inflammatory conditions, butyrate functions as a crucial vita-PAMP that communicates bacterial viability (Mourao-Sa et al., 2013). This vita-PAMP activity of butyrate is most likely attributable to its capacity to block HDACs. Selective inhibition of HDACs, such as HDACs 1-3 and 10, mimicked the effects of butyrate on the modulation of the cytokine response induced by LPS. In particular, IL-10 levels in HDACi-treated macrophages were as low as those in butyrate-treated macrophages. Furthermore, the combined knockdown of HDAC 1-3 resulted in a reduction of IL-10 levels in the presence of the TLR-4 agonist LPS, suggesting a potential role in IL-10 regulation through the inhibition of these HDACs during inflammatory conditions. Moreover, single HDAC knockdown did not reduce IL-10 levels after LPS stimulation likewise, indicating that the butyrate's mode of action mechanism is not attributed to a single HDAC inhibition.

Notably, a knockdown of HDAC 8 alone followed by LPS stimulation resulted in an increase in IL-10 levels compared to the scrambled control in hMDM. One possible explanation for the increase in IL-10 lies in the differential control model described above. It was described previously that the selective HDAC 8 inhibitor PCI-34051 decreased IL-1β in LPS-stimulated PBMC from rheumatoid arthritis (RA) patients by 60 % (Balasubramanian et al., 2008). The differential control model would imply an increase in IL-10 levels following HDAC 8 knockdown and stimulation with LPS which was observed here.

4.4 Butyrate blocks nuclear and mitochondrial STAT3 phosphorylation

Since IL-10 is the most important cytokine in suppressing pro-inflammatory responses in all kinds of autoimmune diseases and limits excessive immune responses, the effect of the SCFA butyrate on the downstream signaling of IL-10 was investigated. STAT3, a key downstream mediator within the IL-10 signaling cascade, is phosphorylated upon IL-10 recognition. This phosphorylation occurs specifically at the Tyr705 (Y705) residue, leading to nuclear translocation of STAT3, where it exerts its role as a transcription factor. Additionally, phosphorylation at Ser727 (S727) induces STAT3 translocation to the mitochondria (mito-STAT3), impacting both mitochondrial metabolism and the generation of reactive oxygen species (ROS) (Balic et al., 2020).

The current study identified that the phosphorylation of both, mitochondrial and nuclear STAT3, was inhibited by butyrate in hMDMs. HDACi, targeting class I HDACs (HDAC 1-3) were able to mimic this effect, suggesting a selective HDAC 1-3 inhibition by butyrate. The importance of STAT3 Tyr705 residue phosphorylation upon IL-10 signaling and subsequent nuclear translocation becomes clear when considering that STAT3 activates effector genes that subsequently repress pro-inflammatory genes mainly at transcriptional level (Hutchins et al., 2013). As a consequence of the blockade of STAT3 phosphorylation by butyrate through IL-10 inhibition observed here, the anti-inflammatory effect of IL-10 is lost. Consequently, this underlines the context-dependent effect of the SCFA butyrate on macrophages, switching from an anti-inflammatory phenotype under steady state conditions to a pro-inflammatory phenotype under inflammatory conditions.

Next to the nuclear STAT3-Tyr705, the phosphorylation of the mito-STAT3 (STAT3-Ser727) was completely inhibited in GM-CSF macrophages upon butyrate administration.

This effect was recapitulated by HDACi with varying specificity. By affecting mitochondrial metabolism and ROS generation, mito-STAT3 is important in generating a metabolic reprogramming in macrophages upon TLR4 signaling (Balic et al., 2020). These changes are necessary for the increased demand of biosynthetic substrates for lipids, proteins and nucleic acids, as well as the increased energy requirements in the inflammatory state (Garaude, 2019; Mills et al., 2016; Van den Bossche et al., 2017). It has been observed that there is reduced production of pro-inflammatory metabolites and inflammation in macrophages that fail to phosphorylate STAT3 Ser727 mediated by a serine to alanine mutation (S727A) (Balic et al., 2020). Nonetheless, we were able to detect high levels of IL-1β secretion upon stimulation with butyrate and LPS and subsequent loss of mito-STAT3 phosphorylation. Hence it would be interesting to study macrophage metabolic reprogramming e.g. in seahorse assay in future follow-up experiments.

Next, it was shown that HDAC inhibitors with varying specificities also abolished the phosphorylation of both nuclear and mitochondrial STAT3 supporting the HDAC inhibitory activity of butyrate. Besides the removal of acetyl groups from lysine residues of histone proteins, HDACs are also involved in the deacetylation of non-histone proteins such as STAT3 (Choudhary et al., 2009). The exact mechanism of HDAC-mediated regulation of STAT3 phosphorylation is still unclear and requires further investigation. One hypothesis is that when HDAC enzymes are inhibited, there is an increase in acetylation of STAT3, which affects its structure, particularly at its phosphorylation sites preventing its phosphorylation by kinases (Gupta et al., 2012).

Interestingly, this study showed that the most potent HDACi inhibiting HDAC 11, namely SIS-17, did not suppress the LPS-mediated STAT3 phosphorylation, and GM-CSF macrophages co-stimulated with SIS 17 and LPS resulted in elevated IL-10 levels, suggesting an HDAC 11 independent mode of action of butyrate. Additionally, HDAC 11 is known as negative regulator of IL-10, when there is an absence of the negative regulation of HDAC11 on IL-10, an increase in IL-10 is to be expected which supports the present data (Villagra et al., 2009).

4.5 Limitations of the experimental approach and future perspective

Although this study provides valuable insights into the effects of butyrate on macrophage-mediated immune responses, several limitations of the experimental design must be

considered. First, the use of in vitro differentiated macrophages from monocytes and LPS stimulation provides a simplified model of the immune response that does not fully recapitulate the complexity of the human GIT. Although this model allows us to study specific molecular interactions in a controlled environment, it lacks the intricate cellular interactions that occur *in vivo*, such as those between epithelial cells, immune cells and the microbiome. In addition, the LPS stimulation used in these experiments is a well-established method of inducing inflammation, but may not fully mimic the diverse range of stimuli encountered in the human GIT during IBD. Therefore, the generalizability of these findings to *in vivo* conditions is limited.

The use of *in vitro* macrophage models and artificial stimulation with butyrate and LPS, while valuable for exploring molecular mechanisms, do not take into account the dynamic metabolic and immune processes in living organisms and require further investigation in more complex, physiologically relevant settings. Future studies using *ex vivo* or *in vivo* models will be essential to validate the therapeutic potential of butyrate in IBD, particularly to define its role in different disease stages and under varying inflammatory conditions, such as *ex vivo* stimulation of intestinal biopsies or PBMCs from IBD patients.

4.6 Conclusion

In conclusion, this study highlights the potent HDAC-inhibitory properties of the bacterial fermentation product butyrate, mainly inhibiting class I HDACs under inflammatory conditions in GM-MDMs *in vitro*. Furthermore, the findings reveal butyrate's capacity to block the release of the anti-inflammatory cytokine IL-10 in a TLR-4 dependent manner. Notably, this inhibitory effect was replicated by HDAC inhibitors with varying specificities, emphasizing the common feature of HDAC inhibition among these compounds. This was further supported by a butyrate-induced H3K27 acetylation. In addition, both butyrate and HDAC inhibitors restricted the downstream signaling of IL-10, effectively inhibiting STAT3 phosphorylation.

These findings elucidate the potential reasons behind the detrimental effects of butyrate treatment during the acute inflammatory phase of IBD, suggesting its potential use in remission and as maintenance therapy.

Future research should aim to further elucidate the interplay between butyrate, HDAC inhibitors and the immune response in the specific context of IBD, with a particular focus

on delineating the ideal treatment regimen at different disease stages. In addition, exploring the underlying mechanisms of butyrate's dual role in both inflammatory and non-inflammatory conditions could provide critical insights into more tailored and effective therapeutic strategies for IBD.

5 Summary

Inflammatory bowel disease (IBD), which includes Crohn's disease and ulcerative colitis, is characterized by chronic inflammation of the gastrointestinal tract. Although the cause of IBD is not uncovered yet, its sharp rise in incidence in the Western world highlights the importance of unraveling its pathogenesis. It is proven that the increasing number of IBD cases is accompanied by a decreased consumption of indigestible starch and fiber. In the human gastrointestinal tract, dietary fiber is fermented by commensal bacteria into short-chain fatty acids (SCFAs), including acetate, propionate and butyrate.

SCFAs were shown to induce anti-inflammatory phenotypes in immune cells and are critical for maintaining intestinal homeostasis. However, once dysbiosis in the gut develops, fiber-rich foods and particularly butyrate can exacerbate IBD pathogenesis. It is also known that mutations of the major anti-inflammatory cytokine IL-10 or its receptor result in early onset IBD highlighting the importance of immune dysregulation on disease development. To date, there is no specific curative treatment available for IBD.

Therefore, the study aims to investigate the impact of the SCFA butyrate on the immune response of macrophages under inflammatory conditions to gain insights into the pathogenesis being relevant for potential novel therapeutic approaches.

To mimic the leaky gut microenvironment under pro-inflammatory conditions during IBD *in vitro*, primary human macrophages are exposed to lipopolysaccharide both in the presence and absence of butyrate. Small interfering RNA-mediated knockdown experiments of histone deacetylase enzymes and exposure of macrophages to histone deacetylase inhibitors with varying specificities are performed to depict the operating principle of butyrate. Protein expression of various cytokines is assessed by homogenous time-resolved fluorescence and gene expression is determined using reverse transcription quantitative real-time PCR. For investigating the genome-wide effect of butyrate, chromatin immunoprecipitation sequencing is performed.

The findings indicate that the SCFA butyrate is a potent inhibitor of histone deacetylase class I enzymes under inflammatory conditions. Moreover, butyrate can inhibit the release of the anti-inflammatory cytokine IL-10 in a toll-like receptor 4-dependent manner. The butyrate’s blockage of IL-10 results in an inhibited downstream phosphorylation of Signal transducer and activator of transcription 3.

Next, this inhibitory effect of butyrate can be mimicked by histone deacetylase inhibitors with varying specificities and an increase of acetylation of histone 3 lysine 27 is observed after butyrate administration in primary human macrophages emphasizing the feature of histone deacetylase inhibition of butyrate. Subsequently, we demonstrated a differential regulation of cytokine expression and inflammatory response in macrophages due to epigenetic reprogramming by butyrate.

These findings elucidate the potential reasons behind the detrimental effects of butyrate treatment during the acute inflammatory phase of IBD, suggesting its potential use in remission and as maintenance therapy. Future studies should seek to provide a deeper understanding of the interaction between butyrate, histone deacetylase inhibitors, and the immune system in the context of IBD, especially focusing on the context-dependent effects of butyrate.

6 List of figures

Figure 1: Diagram of the IL-10 Pathway. 15
Figure 2: Schematic protocol of the knockdown experiment procedure. 34
Figure 3: Schematic protocol of HDAC inhibitor experiments. 36
Figure 4: Knockdown efficiency in primary human GM-CSF macrophages. 44
Figure 5: Effect of single HDAC knockdown on IL-10 secretion. 46
Figure 6: Effect of HDAC inhibitors on histone acetylation and cytokine levels. 48
Figure 7: Butyrate blocks IL-10 expression on the transcriptional level. 50
Figure 8: siRNA mediated HDAC1-3 knockdown. 52
Figure 9: Butyrate inhibits STAT3 signaling via HDAC inhibition. 54
Figure 10: H3K27 Acetylation status. 55

7 List of tables

Table 1: List of short-chain fatty acids 19
Table 2: List of primary antibodies 29
Table 3: List of secondary antibodies used for Western blot 29
Table 4: List of siRNAs used for electroporation 30
Table 5: List of qPCR primers used for amplification of human genes 30
Table 6: List of cell culture medium 31
Table 7: List of buffers and solutions 31
Table 8: List of HDAC inhibitors and working concentrations 36
Table 9: Thermal cycler settings for qPCR experiments 38
Table 10: Settings WES 40

8 References

Abegunde, AT, Muhammad, BH, Bhatti, O, Ali, T. Environmental risk factors for inflammatory bowel diseases: Evidence based literature review. World J Gastroenterol 2016; 22: 6296-6317

Ananthakrishnan, AN, Khalili, H, Konijeti, GG, Higuchi, LM, de Silva, P, Korzenik, JR, Fuchs, CS, Willett, WC, Richter, JM, Chan, AT. A prospective study of long-term intake of dietary fiber and risk of Crohn's disease and ulcerative colitis. Gastroenterology 2013; 145: 970-977

Ashton, JJ, Seaby, EG, Beattie, RM, Ennis, S. NOD2 in Crohn's Disease-Unfinished Business. J Crohns Colitis 2023; 17: 450-458

Bain, CC, Scott, CL, Uronen-Hansson, H, Gudjonsson, S, Jansson, O, Grip, O, Guilliams, M, Malissen, B, Agace, WW, Mowat, AM. Resident and pro-inflammatory macrophages in the colon represent alternative context-dependent fates of the same Ly6Chi monocyte precursors. Mucosal Immunol 2013; 6: 498-510

Balasubramanian, S, Ramos, J, Luo, W, Sirisawad, M, Verner, E, Buggy, JJ. A novel histone deacetylase 8 (HDAC8)-specific inhibitor PCI-34051 induces apoptosis in T-cell lymphomas. Leukemia 2008; 22: 1026-1034

Balic, JJ, Albargy, H, Luu, K, Kirby, FJ, Jayasekara, WSN, Mansell, F, Garama, DJ, De Nardo, D, Baschuk, N, Louis, C, Humphries, F, Fitzgerald, K, Latz, E, Gough, DJ, Mansell, A. STAT3 serine phosphorylation is required for TLR4 metabolic reprogramming and IL-1beta expression. Nat Commun 2020; 11: 3816-3827

Bassaganya-Riera, J, DiGuardo, M, Viladomiu, M, de Horna, A, Sanchez, S, Einerhand, AW, Sanders, L, Hontecillas, R. Soluble fibers and resistant starch ameliorate disease activity in interleukin-10-deficient mice with inflammatory bowel disease. J Nutr 2011; 141: 1318-1325

Bian, F, Xiao, Y, Zaheer, M, Volpe, EA, Pflugfelder, SC, Li, DQ, de Paiva, CS. Inhibition of NLRP3 Inflammasome Pathway by Butyrate Improves Corneal Wound Healing in Corneal Alkali Burn. Int J Mol Sci 2017; 18: 562-576

Bosi, E, Molteni, L, Radaelli, MG, Folini, L, Fermo, I, Bazzigaluppi, E, Piemonti, L, Pastore, MR, Paroni, R. Increased intestinal permeability precedes clinical onset of type 1 diabetes. Diabetologia 2006; 49: 2824-2827

Bours, MJ, Swennen, EL, Di Virgilio, F, Cronstein, BN, Dagnelie, PC. Adenosine 5'-triphosphate and adenosine as endogenous signaling molecules in immunity and inflammation. Pharmacol Ther 2006; 112: 358-404

Brown, AJ, Goldsworthy, SM, Barnes, AA, Eilert, MM, Tcheang, L, Daniels, D, Muir, AI, Wigglesworth, MJ, Kinghorn, I, Fraser, NJ, Pike, NB, Strum, JC, Steplewski, KM, Murdock, PR, Holder, JC, Marshall, FH, Szekeres, PG, Wilson, S, Ignar, DM, Foord, SM, Wise, A, Dowell, SJ. The Orphan G protein-coupled receptors GPR41 and GPR43 are activated by propionate and other short chain carboxylic acids. J Biol Chem 2003; 278: 11312-11319

Caetano, MAF, Castelucci, P. Role of short chain fatty acids in gut health and possible therapeutic approaches in inflammatory bowel diseases. World J Clin Cases 2022; 10: 9985-10003

Cassioli, C, Baldari, CT. The Expanding Arsenal of Cytotoxic T Cells. Front Immunol 2022; 13: 883010

Chang, EY, Guo, B, Doyle, SE, Cheng, G. Cutting edge: involvement of the type I IFN production and signaling pathway in lipopolysaccharide-induced IL-10 production. J Immunol 2007; 178: 6705-6709

Chang, PV, Hao, L, Offermanns, S, Medzhitov, R. The microbial metabolite butyrate regulates intestinal macrophage function via histone deacetylase inhibition. Proc Natl Acad Sci U S A 2014; 111: 2247-2252

Chanteux, H, Guisset, AC, Pilette, C, Sibille, Y. LPS induces IL-10 production by human alveolar macrophages via MAPKinases- and Sp1-dependent mechanisms. Respir Res 2007; 8: 71

Chen, GY, Nunez, G. Sterile inflammation: sensing and reacting to damage. Nat Rev Immunol 2010; 10: 826-837

Choudhary, C, Kumar, C, Gnad, F, Nielsen, ML, Rehman, M, Walther, TC, Olsen, JV, Mann, M. Lysine acetylation targets protein complexes and co-regulates major cellular functions. Science 2009; 325: 834-840

Chuenchor, W, Jin, T, Ravilious, G, Xiao, TS. Structures of pattern recognition receptors reveal molecular mechanisms of autoinhibition, ligand recognition and oligomerization. Curr Opin Immunol 2014; 26: 14-20

Cox, MA, Jackson, J, Stanton, M, Rojas-Triana, A, Bober, L, Laverty, M, Yang, X, Zhu, F, Liu, J, Wang, S, Monsma, F, Vassileva, G, Maguire, M, Gustafson, E, Bayne, M, Chou, CC, Lundell, D, Jenh, CH. Short-chain fatty acids act as antiinflammatory mediators by regulating prostaglandin E(2) and cytokines. World J Gastroenterol 2009; 15: 5549-5557

Croker, BA, Krebs, DL, Zhang, JG, Wormald, S, Willson, TA, Stanley, EG, Robb, L, Greenhalgh, CJ, Forster, I, Clausen, BE, Nicola, NA, Metcalf, D, Hilton, DJ, Roberts, AW, Alexander, WS. SOCS3 negatively regulates IL-6 signaling in vivo. Nat Immunol 2003; 4: 540-545

Cummings, JH, Pomare, EW, Branch, WJ, Naylor, CP, Macfarlane, GT. Short chain fatty acids in human large intestine, portal, hepatic and venous blood. Gut 1987; 28: 1221-1227

Dalile, B, Van Oudenhove, L, Vervliet, B, Verbeke, K. The role of short-chain fatty acids in microbiota-gut-brain communication. Nat Rev Gastroenterol Hepatol 2019; 16: 461-478

de Lange, KM, Moutsianas, L, Lee, JC, Lamb, CA, Luo, Y, Kennedy, NA, Jostins, L, Rice, DL, Gutierrez-Achury, J, Ji, SG, Heap, G, Nimmo, ER, Edwards, C, Henderson, P, Mowat, C, Sanderson, J, Satsangi, J, Simmons, A, Wilson, DC, Tremelling, M, Hart, A, Mathew, CG, Newman, WG, Parkes, M, Lees, CW, Uhlig, H, Hawkey, C, Prescott, NJ, Ahmad, T, Mansfield, JC, Anderson, CA, Barrett, JC. Genome-wide association study implicates immune activation of multiple integrin genes in inflammatory bowel disease. Nat Genet 2017; 49: 256-261

Eckschlager, T, Plch, J, Stiborova, M, Hrabeta, J. Histone Deacetylase Inhibitors as Anticancer Drugs. Int J Mol Sci 2017; 18: 1414-1439

Facchin, S, Vitulo, N, Calgaro, M, Buda, A, Romualdi, C, Pohl, D, Perini, B, Lorenzon, G, Marinelli, C, D'Inca, R, Sturniolo, GC, Savarino, EV. Microbiota changes induced by microencapsulated sodium butyrate in patients with inflammatory bowel disease. Neurogastroenterol Motil 2020; 32: e13914

Fasano, A, Not, T, Wang, W, Uzzau, S, Berti, I, Tommasini, A, Goldblum, SE. Zonulin, a newly discovered modulator of intestinal permeability, and its expression in coeliac disease. Lancet 2000; 355: 1518-1519

Finbloom, DS, Winestock, KD. IL-10 induces the tyrosine phosphorylation of tyk2 and Jak1 and the differential assembly of STAT1 alpha and STAT3 complexes in human T cells and monocytes. J Immunol 1995; 155: 1079-1090

Flajnik, MF, Kasahara, M. Origin and evolution of the adaptive immune system: genetic events and selective pressures. Nat Rev Genet 2010; 11: 47-59

Garaude, J. Reprogramming of mitochondrial metabolism by innate immunity. Curr Opin Immunol 2019; 56: 17-23

Gearry, RB, Irving, PM, Barrett, JS, Nathan, DM, Shepherd, SJ, Gibson, PR. Reduction of dietary poorly absorbed short-chain carbohydrates (FODMAPs) improves abdominal symptoms in patients with inflammatory bowel disease-a pilot study. J Crohns Colitis 2009; 3: 8-14

Genser, L, Aguanno, D, Soula, HA, Dong, L, Trystram, L, Assmann, K, Salem, JE, Vaillant, JC, Oppert, JM, Laugerette, F, Michalski, MC, Wind, P, Rousset, M, Brot-Laroche, E, Leturque, A, Clement, K, Thenet, S, Poitou, C. Increased jejunal permeability in human obesity is revealed by a lipid challenge and is linked to inflammation and type 2 diabetes. J Pathol 2018; 246: 217-230

Gierynska, M, Szulc-Dabrowska, L, Struzik, J, Mielcarska, MB, Gregorczyk-Zboroch, KP. Integrity of the Intestinal Barrier: The Involvement of Epithelial Cells and Microbiota-A Mutual Relationship. Animals (Basel) 2022; 12: 145-177

Glauben, R, Batra, A, Fedke, I, Zeitz, M, Lehr, HA, Leoni, F, Mascagni, P, Fantuzzi, G, Dinarello, CA, Siegmund, B. Histone hyperacetylation is associated with amelioration of experimental colitis in mice. J Immunol 2006; 176: 5015-5022

Goto, Y. Epithelial Cells as a Transmitter of Signals From Commensal Bacteria and Host Immune Cells. Front Immunol 2019; 10: 2057

Graham, DB, Xavier, RJ. Pathway paradigms revealed from the genetics of inflammatory bowel disease. Nature 2020; 578: 527-539

Groschwitz, KR, Hogan, SP. Intestinal barrier function: molecular regulation and disease pathogenesis. J Allergy Clin Immunol 2009; 124: 3-20

Gupta, M, Han, JJ, Stenson, M, Wellik, L, Witzig, TE. Regulation of STAT3 by histone deacetylase-3 in diffuse large B-cell lymphoma: implications for therapy. Leukemia 2012; 26: 1356-1364

Hanning, N, Edwinson, AL, Ceuleers, H, Peters, SA, De Man, JG, Hassett, LC, De Winter, BY, Grover, M. Intestinal barrier dysfunction in irritable bowel syndrome: a systematic review. Therap Adv Gastroenterol 2021; 14: 1756284821993586

Heaney, LM. Applying mass spectrometry-based assays to explore gut microbial metabolism and associations with disease. Clin Chem Lab Med 2020; 58: 719-732

Hodgkinson, K, El Abbar, F, Dobranowski, P, Manoogian, J, Butcher, J, Figeys, D, Mack, D, Stintzi, A. Butyrate's role in human health and the current progress towards its clinical application to treat gastrointestinal disease. Clin Nutr 2023; 42: 61-75

Hoffman, W, Lakkis, FG, Chalasani, G. B Cells, Antibodies, and More. Clin J Am Soc Nephrol 2016; 11: 137-154

Hontecillas-Prieto, L, Flores-Campos, R, Silver, A, de Alava, E, Hajji, N, Garcia-Dominguez, DJ. Synergistic Enhancement of Cancer Therapy Using HDAC Inhibitors: Opportunity for Clinical Trials. Front Genet 2020; 11: 578011

Huang, B, Li, G, Jiang, XH. Fate determination in mesenchymal stem cells: a perspective from histone-modifying enzymes. Stem Cell Res Ther 2015; 6: 35

Hutchins, AP, Diez, D, Miranda-Saavedra, D. The IL-10/STAT3-mediated anti-inflammatory response: recent developments and future challenges. Brief Funct Genomics 2013; 12: 489-498

Imhann, F, Vich Vila, A, Bonder, MJ, Fu, J, Gevers, D, Visschedijk, MC, Spekhorst, LM, Alberts, R, Franke, L, van Dullemen, HM, Ter Steege, RWF, Huttenhower, C, Dijkstra, G, Xavier, RJ, Festen, EAM, Wijmenga, C, Zhernakova, A, Weersma, RK. Interplay of host genetics and gut microbiota underlying the onset and clinical presentation of inflammatory bowel disease. Gut 2018; 67: 108-119

Iwasaki, A, Medzhitov, R. Control of adaptive immunity by the innate immune system. Nat Immunol 2015; 16: 343-353

Iyer, SS, Cheng, G. Role of interleukin 10 transcriptional regulation in inflammation and autoimmune disease. Crit Rev Immunol 2012; 32: 23-63

Jiang, L, Wang, J, Liu, Z, Jiang, A, Li, S, Wu, D, Zhang, Y, Zhu, X, Zhou, E, Wei, Z, Yang, Z. Sodium Butyrate Alleviates Lipopolysaccharide-Induced Inflammatory Responses by Down-Regulation of NF-kappaB, NLRP3 Signaling Pathway, and Activating Histone Acetylation in Bovine Macrophages. Front Vet Sci 2020; 7: 579674

Kawai, T, Akira, S. The roles of TLRs, RLRs and NLRs in pathogen recognition. Int Immunol 2009; 21: 317-337

Kawai, T, Akira, S. Toll-like receptors and their crosstalk with other innate receptors in infection and immunity. Immunity 2011; 34: 637-650

Kawai, T, Takeuchi, O, Fujita, T, Inoue, J, Muhlradt, PF, Sato, S, Hoshino, K, Akira, S. Lipopolysaccharide stimulates the MyD88-independent pathway and results in activation of IFN-regulatory factor 3 and the expression of a subset of lipopolysaccharide-inducible genes. J Immunol 2001; 167: 5887-5894

Kondelkova, K, Vokurkova, D, Krejsek, J, Borska, L, Fiala, Z, Ctirad, A. Regulatory T cells (TREG) and their roles in immune system with respect to immunopathological disorders. Acta Medica (Hradec Kralove) 2010; 53: 73-77

Kono, H, Chen, CJ, Ontiveros, F, Rock, KL. Uric acid promotes an acute inflammatory response to sterile cell death in mice. J Clin Invest 2010; 120: 1939-1949

Kotenko, SV, Krause, CD, Izotova, LS, Pollack, BP, Wu, W, Pestka, S. Identification and functional characterization of a second chain of the interleukin-10 receptor complex. EMBO J 1997; 16: 5894-5903

Kuhn, R, Lohler, J, Rennick, D, Rajewsky, K, Muller, W. Interleukin-10-deficient mice develop chronic enterocolitis. Cell 1993; 75: 263-274

Lang, R, Pauleau, AL, Parganas, E, Takahashi, Y, Mages, J, Ihle, JN, Rutschman, R, Murray, PJ. SOCS3 regulates the plasticity of gp130 signaling. Nat Immunol 2003; 4: 546-550

Latz, E, Xiao, TS, Stutz, A. Activation and regulation of the inflammasomes. Nat Rev Immunol 2013; 13: 397-411

Le Poul, E, Loison, C, Struyf, S, Springael, JY, Lannoy, V, Decobecq, ME, Brezillon, S, Dupriez, V, Vassart, G, Van Damme, J, Parmentier, M, Detheux, M. Functional characterization of human receptors for short chain fatty acids and their role in polymorphonuclear cell activation. J Biol Chem 2003; 278: 25481-25489

Li, D, Wu, M. Pattern recognition receptors in health and diseases. Signal Transduct Target Ther 2021; 6: 291

Littman, DR, Pamer, EG. Role of the commensal microbiota in normal and pathogenic host immune responses. Cell Host Microbe 2011; 10: 311-323

Louis, P, Hold, GL, Flint, HJ. The gut microbiota, bacterial metabolites and colorectal cancer. Nat Rev Microbiol 2014; 12: 661-672

Luckheeram, RV, Zhou, R, Verma, AD, Xia, B. CD4(+)T cells: differentiation and functions. Clin Dev Immunol 2012; 2012: 925135

Maagaard, L, Ankersen, DV, Vegh, Z, Burisch, J, Jensen, L, Pedersen, N, Munkholm, P. Follow-up of patients with functional bowel symptoms treated with a low FODMAP diet. World J Gastroenterol 2016; 22: 4009-4019

Madsen, KL, Doyle, JS, Tavernini, MM, Jewell, LD, Rennie, RP, Fedorak, RN. Antibiotic therapy attenuates colitis in interleukin 10 gene-deficient mice. Gastroenterology 2000; 118: 1094-1105

Mankertz, J, Schulzke, JD. Altered permeability in inflammatory bowel disease: pathophysiology and clinical implications. Curr Opin Gastroenterol 2007; 23: 379-383

Marchesi, JR, Holmes, E, Khan, F, Kochhar, S, Scanlan, P, Shanahan, F, Wilson, ID, Wang, Y. Rapid and noninvasive metabonomic characterization of inflammatory bowel disease. J Proteome Res 2007; 6: 546-551

Marks, PA, Richon, VM, Miller, T, Kelly, WK. Histone deacetylase inhibitors. Adv Cancer Res 2004; 91: 137-168

Marshall, JS, Warrington, R, Watson, W, Kim, HL. An introduction to immunology and immunopathology. Allergy Asthma Clin Immunol 2018; 14: 49

Martin, R, Miquel, S, Ulmer, J, Kechaou, N, Langella, P, Bermudez-Humaran, LG. Role of commensal and probiotic bacteria in human health: a focus on inflammatory bowel disease. Microb Cell Fact 2013; 12: 71

Martinez, C, Lobo, B, Pigrau, M, Ramos, L, Gonzalez-Castro, AM, Alonso, C, Guilarte, M, Guila, M, de Torres, I, Azpiroz, F, Santos, J, Vicario, M. Diarrhoea-predominant irritable bowel syndrome: an organic disorder with structural abnormalities in the jejunal epithelial barrier. Gut 2013; 62: 1160-1168

Martini, E, Krug, SM, Siegmund, B, Neurath, MF, Becker, C. Mend Your Fences: The Epithelial Barrier and its Relationship With Mucosal Immunity in Inflammatory Bowel Disease. Cell Mol Gastroenterol Hepatol 2017; 4: 33-46

Meissner, F, Scheltema, RA, Mollenkopf, HJ, Mann, M. Direct proteomic quantification of the secretome of activated immune cells. Science 2013; 340: 475-478

Milazzo, G, Mercatelli, D, Di Muzio, G, Triboli, L, De Rosa, P, Perini, G, Giorgi, FM. Histone Deacetylases (HDACs): Evolution, Specificity, Role in Transcriptional Complexes, and Pharmacological Actionability. Genes (Basel) 2020; 11: 556-605

Mills, EL, Kelly, B, Logan, A, Costa, ASH, Varma, M, Bryant, CE, Tourlomousis, P, Dabritz, JHM, Gottlieb, E, Latorre, I, Corr, SC, McManus, G, Ryan, D, Jacobs, HT, Szibor, M, Xavier, RJ, Braun, T, Frezza, C, Murphy, MP, O'Neill, LA. Succinate Dehydrogenase Supports Metabolic Repurposing of Mitochondria to Drive Inflammatory Macrophages. Cell 2016; 167: 457-470

Miyoshi, J, Chang, EB. The gut microbiota and inflammatory bowel diseases. Transl Res 2017; 179: 38-48

Mogensen, TH. Pathogen recognition and inflammatory signaling in innate immune defenses. Clin Microbiol Rev 2009; 22: 240-273

Mohajeri, MH, Brummer, RJM, Rastall, RA, Weersma, RK, Harmsen, HJM, Faas, M, Eggersdorfer, M. The role of the microbiome for human health: from basic science to clinical applications. Eur J Nutr 2018; 57: 1-14

Mondot, S, de Wouters, T, Dore, J, Lepage, P. The human gut microbiome and its dysfunctions. Dig Dis 2013; 31: 278-285

Moran, CJ, Walters, TD, Guo, CH, Kugathasan, S, Klein, C, Turner, D, Wolters, VM, Bandsma, RH, Mouzaki, M, Zachos, M, Langer, JC, Cutz, E, Benseler, SM, Roifman, CM, Silverberg, MS, Griffiths, AM, Snapper, SB, Muise, AM. IL-10R polymorphisms are associated with very-early-onset ulcerative colitis. Inflamm Bowel Dis 2013; 19: 115-123

Motta, V, Soares, F, Sun, T, Philpott, DJ. NOD-like receptors: versatile cytosolic sentinels. Physiol Rev 2015; 95: 149-178

Mourao-Sa, D, Roy, S, Blander, JM. Vita-PAMPs: signatures of microbial viability. Adv Exp Med Biol 2013; 785: 1-8

Mowat, AM. To respond or not to respond - a personal perspective of intestinal tolerance. Nat Rev Immunol 2018; 18: 405-415

Mowat, AM, Agace, WW. Regional specialization within the intestinal immune system. Nat Rev Immunol 2014; 14: 667-685

Mueller, SN, Gebhardt, T, Carbone, FR, Heath, WR. Memory T cell subsets, migration patterns, and tissue residence. Annu Rev Immunol 2013; 31: 137-161

Murray, PJ. The primary mechanism of the IL-10-regulated antiinflammatory response is to selectively inhibit transcription. Proc Natl Acad Sci U S A 2005; 102: 8686-8691

Murray, PJ. STAT3-mediated anti-inflammatory signalling. Biochem Soc Trans 2006; 34: 1028-1031

Murray, PJ. The JAK-STAT signaling pathway: input and output integration. J Immunol 2007; 178: 2623-2629

Neurath, MF. Cytokines in inflammatory bowel disease. Nat Rev Immunol 2014; 14: 329-342

Ney, LM, Wipplinger, M, Grossmann, M, Engert, N, Wegner, VD, Mosig, AS. Short chain fatty acids: key regulators of the local and systemic immune response in inflammatory diseases and infections. Open Biol 2023; 13: 230014

Ng, SC, Shi, HY, Hamidi, N, Underwood, FE, Tang, W, Benchimol, EI, Panaccione, R, Ghosh, S, Wu, JCY, Chan, FKL, Sung, JJY, Kaplan, GG. Worldwide incidence and prevalence of inflammatory bowel disease in the 21st century: a systematic review of population-based studies. Lancet 2017; 390: 2769-2778

Nguyen, LH, Ortqvist, AK, Cao, Y, Simon, TG, Roelstraete, B, Song, M, Joshi, AD, Staller, K, Chan, AT, Khalili, H, Olen, O, Ludvigsson, JF. Antibiotic use and the development of inflammatory bowel disease: a national case-control study in Sweden. Lancet Gastroenterol Hepatol 2020; 5: 986-995

Nishida, A, Inoue, R, Inatomi, O, Bamba, S, Naito, Y, Andoh, A. Gut microbiota in the pathogenesis of inflammatory bowel disease. Clin J Gastroenterol 2018; 11: 1-10

Parada Venegas, D, De la Fuente, MK, Landskron, G, Gonzalez, MJ, Quera, R, Dijkstra, G, Harmsen, HJM, Faber, KN, Hermoso, MA. Short Chain Fatty Acids (SCFAs)-Mediated Gut Epithelial and Immune Regulation and Its Relevance for Inflammatory Bowel Diseases. Front Immunol 2019; 10: 277

Park, OJ, Ha, YE, Sim, JR, Lee, D, Lee, EH, Kim, SY, Yun, CH, Han, SH. Butyrate potentiates Enterococcus faecalis lipoteichoic acid-induced inflammasome activation via histone deacetylase inhibition. Cell Death Discov 2023; 9: 107

Pisani, A, Rausch, P, Bang, C, Ellul, S, Tabone, T, Marantidis Cordina, C, Zahra, G, Franke, A, Ellul, P. Dysbiosis in the Gut Microbiota in Patients with Inflammatory Bowel Disease during Remission. Microbiol Spectr 2022; 10: e00616-00622

Qin, J, Li, R, Raes, J, Arumugam, M, Burgdorf, KS, Manichanh, C, Nielsen, T, Pons, N, Levenez, F, Yamada, T, Mende, DR, Li, J, Xu, J, Li, S, Li, D, Cao, J, Wang, B, Liang, H, Zheng, H, Xie, Y, Tap, J, Lepage, P, Bertalan, M, Batto, JM, Hansen, T, Le Paslier, D, Linneberg, A, Nielsen, HB, Pelletier, E, Renault, P, Sicheritz-Ponten, T, Turner, K, Zhu, H, Yu, C, Li, S, Jian, M, Zhou, Y, Li, Y, Zhang, X, Li, S, Qin, N, Yang, H, Wang, J, Brunak, S, Dore, J, Guarner, F, Kristiansen, K, Pedersen, O, Parkhill, J, Weissenbach, J, Meta, HITC, Bork, P, Ehrlich, SD, Wang, J. A human gut microbial gene catalogue established by metagenomic sequencing. Nature 2010; 464: 59-65

Quintana, FJ, Cohen, IR. Heat shock proteins as endogenous adjuvants in sterile and septic inflammation. J Immunol 2005; 175: 2777-2782

Ramos, GP, Papadakis, KA. Mechanisms of Disease: Inflammatory Bowel Diseases. Mayo Clin Proc 2019; 94: 155-165

Riera Romo, M, Perez-Martinez, D, Castillo Ferrer, C. Innate immunity in vertebrates: an overview. Immunology 2016; 148: 125-139

Rizzello, F, Spisni, E, Giovanardi, E, Imbesi, V, Salice, M, Alvisi, P, Valerii, MC, Gionchetti, P. Implications of the Westernized Diet in the Onset and Progression of IBD. Nutrients 2019; 11: 1033-1057

Russo, E, Giudici, F, Fiorindi, C, Ficari, F, Scaringi, S, Amedei, A. Immunomodulating Activity and Therapeutic Effects of Short Chain Fatty Acids and Tryptophan Post-biotics in Inflammatory Bowel Disease. Front Immunol 2019; 10: 2754

Salvi, PS, Cowles, RA. Butyrate and the Intestinal Epithelium: Modulation of Proliferation and Inflammation in Homeostasis and Disease. Cells 2021; 10: 1775-1788

Sange, AH, Srinivas, N, Sarnaik, MK, Modi, S, Pisipati, Y, Vaidya, S, Syed Gaggatur, N, Sange, I. Extra-Intestinal Manifestations of Inflammatory Bowel Disease. Cureus 2021; 13: e17187

Santana, PT, Rosas, SLB, Ribeiro, BE, Marinho, Y, de Souza, HSP. Dysbiosis in Inflammatory Bowel Disease: Pathogenic Role and Potential Therapeutic Targets. Int J Mol Sci 2022; 23: 3464-3489

Scheppach, W. Treatment of distal ulcerative colitis with short-chain fatty acid enemas. A placebo-controlled trial. German-Austrian SCFA Study Group. Dig Dis Sci 1996; 41: 2254-2259

Schulthess, J, Pandey, S, Capitani, M, Rue-Albrecht, KC, Arnold, I, Franchini, F, Chomka, A, Ilott, NE, Johnston, DGW, Pires, E, McCullagh, J, Sansom, SN, Arancibia-Carcamo, CV, Uhlig, HH, Powrie, F. The Short Chain Fatty Acid Butyrate Imprints an Antimicrobial Program in Macrophages. Immunity 2019; 50: 432-445

Seyedian, SS, Nokhostin, F, Malamir, MD. A review of the diagnosis, prevention, and treatment methods of inflammatory bowel disease. J Med Life 2019; 12: 113-122

Shouval, DS, Biswas, A, Goettel, JA, McCann, K, Conaway, E, Redhu, NS, Mascanfroni, ID, Al Adham, Z, Lavoie, S, Ibourk, M, Nguyen, DD, Samsom, JN, Escher, JC, Somech, R, Weiss, B, Beier, R, Conklin, LS, Ebens, CL, Santos, FG, Ferreira, AR, Sherlock, M, Bhan, AK, Muller, W, Mora, JR, Quintana, FJ, Klein, C, Muise, AM, Horwitz, BH, Snapper, SB. Interleukin-10 receptor signaling in innate immune cells regulates mucosal immune tolerance and anti-inflammatory macrophage function. Immunity 2014; 40: 706-719

Siddiqui, MT, Cresci, GAM. The Immunomodulatory Functions of Butyrate. J Inflamm Res 2021; 14: 6025-6041

Smythies, LE, Sellers, M, Clements, RH, Mosteller-Barnum, M, Meng, G, Benjamin, WH, Orenstein, JM, Smith, PD. Human intestinal macrophages display profound inflammatory anergy despite avid phagocytic and bacteriocidal activity. J Clin Invest 2005; 115: 66-75

Steinhart, AH, Hiruki, T, Brzezinski, A, Baker, JP. Treatment of left-sided ulcerative colitis with butyrate enemas: a controlled trial. Aliment Pharmacol Ther 1996; 10: 729-736

Steliou, K, Boosalis, MS, Perrine, SP, Sangerman, J, Faller, DV. Butyrate histone deacetylase inhibitors. Biores Open Access 2012; 1: 192-198

Stolfi, C, Maresca, C, Monteleone, G, Laudisi, F. Implication of Intestinal Barrier Dysfunction in Gut Dysbiosis and Diseases. Biomedicines 2022; 10: 289-318

Tan, JC, Indelicato, SR, Narula, SK, Zavodny, PJ, Chou, CC. Characterization of interleukin-10 receptors on human and mouse cells. J Biol Chem 1993; 268: 21053-21059

Thangaraju, M, Cresci, GA, Liu, K, Ananth, S, Gnanaprakasam, JP, Browning, DD, Mellinger, JD, Smith, SB, Digby, GJ, Lambert, NA, Prasad, PD, Ganapathy, V. GPR109A is a G-protein-coupled receptor for the bacterial fermentation product butyrate and functions as a tumor suppressor in colon. Cancer Res 2009; 69: 2826-2832

Ueda, Y, Kayama, H, Jeon, SG, Kusu, T, Isaka, Y, Rakugi, H, Yamamoto, M, Takeda, K. Commensal microbiota induce LPS hyporesponsiveness in colonic macrophages via the production of IL-10. Int Immunol 2010; 22: 953-962

Valitutti, F, Cucchiara, S, Fasano, A. Celiac Disease and the Microbiome. Nutrients 2019; 11: 2403-2422

Van den Bossche, J, O'Neill, LA, Menon, D. Macrophage Immunometabolism: Where Are We (Going)? Trends Immunol 2017; 38: 395-406

Van Der Kraak, L, Gros, P, Beauchemin, N. Colitis-associated colon cancer: Is it in your genes? World J Gastroenterol 2015; 21: 11688-11699

Vancamelbeke, M, Vermeire, S. The intestinal barrier: a fundamental role in health and disease. Expert Rev Gastroenterol Hepatol 2017; 11: 821-834

Vernero, M, De Blasio, F, Ribaldone, DG, Bugianesi, E, Pellicano, R, Saracco, GM, Astegiano, M, Caviglia, GP. The Usefulness of Microencapsulated Sodium Butyrate Add-On Therapy in Maintaining Remission in Patients with Ulcerative Colitis: A Prospective Observational Study. J Clin Med 2020; 9: 3941-3950

Vijay, A, Valdes, AM. Role of the gut microbiome in chronic diseases: a narrative review. Eur J Clin Nutr 2022; 76: 489-501

Villagra, A, Cheng, F, Wang, HW, Suarez, I, Glozak, M, Maurin, M, Nguyen, D, Wright, KL, Atadja, PW, Bhalla, K, Pinilla-Ibarz, J, Seto, E, Sotomayor, EM. The histone deacetylase HDAC11 regulates the expression of interleukin 10 and immune tolerance. Nat Immunol 2009; 10: 92-100

Wallace, DC, Fan, W. Energetics, epigenetics, mitochondrial genetics. Mitochondrion 2010; 10: 12-31

Wang, W, Dernst, A, Martin, B, Lorenzi, L, Cadefau, M, Phulphag, K, Wagener, A, Budden, C, Stair, N, Wagner, T, Färber, H, Jaensch, A, Stahl, R, Duthie, F, Schmidt, SV, Coll, RC, Meissner, F, Cuartero, S, Mangan, MSJ, Latz, E. Butyrate and propionate are microbial danger signals that activate the NLRP3 inflammasome in human macrophages upon TLR stimulation. Cell Rep 2024; 43: 114736

Wilbers, RH, Westerhof, LB, van Raaij, DR, Bakker, J, Smant, G, Schots, A. Granulocyte-macrophage colony-stimulating factor negatively regulates early IL-10-mediated responses. Future Sci OA 2018; 4: FSO288

Wild, CP. Complementing the genome with an "exposome": the outstanding challenge of environmental exposure measurement in molecular epidemiology. Cancer Epidemiol Biomarkers Prev 2005; 14: 1847-1850

Wilkins, LJ, Monga, M, Miller, AW. Defining Dysbiosis for a Cluster of Chronic Diseases. Sci Rep 2019; 9: 12918

Williams, LM, Ricchetti, G, Sarma, U, Smallie, T, Foxwell, BM. Interleukin-10 suppression of myeloid cell activation--a continuing puzzle. Immunology 2004; 113: 281-292

Xavier, RJ, Podolsky, DK. Unravelling the pathogenesis of inflammatory bowel disease. Nature 2007; 448: 427-434

Yoon, S, Eom, GH. HDAC and HDAC Inhibitor: From Cancer to Cardiovascular Diseases. Chonnam Med J 2016; 52: 1-11

Yuan, X, Wang, L, Bhat, OM, Lohner, H, Li, PL. Differential effects of short chain fatty acids on endothelial Nlrp3 inflammasome activation and neointima formation: Antioxidant action of butyrate. Redox Biol 2018; 16: 21-31

Zhang, Y, Lei, Y, Honarpisheh, M, Kemter, E, Wolf, E, Seissler, J. Butyrate and Class I Histone Deacetylase Inhibitors Promote Differentiation of Neonatal Porcine Islet Cells into Beta Cells. Cells 2021; 10: 3249-3263

Zhu, H, Lei, X, Liu, Q, Wang, Y. Interleukin-10-1082A/G polymorphism and inflammatory bowel disease susceptibility: a meta-analysis based on 17,585 subjects. Cytokine 2013; 61: 146-153

Zhu, L, Shi, T, Zhong, C, Wang, Y, Chang, M, Liu, X. IL-10 and IL-10 Receptor Mutations in Very Early Onset Inflammatory Bowel Disease. Gastroenterology Res 2017; 10: 65-69

Zigmond, E, Bernshtein, B, Friedlander, G, Walker, CR, Yona, S, Kim, KW, Brenner, O, Krauthgamer, R, Varol, C, Muller, W, Jung, S. Macrophage-restricted interleukin-10 receptor deficiency, but not IL-10 deficiency, causes severe spontaneous colitis. Immunity 2014; 40: 720-733

Zindel, J, Kubes, P. DAMPs, PAMPs, and LAMPs in Immunity and Sterile Inflammation. Annu Rev Pathol 2020; 15: 493-518

9 Statement on own contribution

The study was conducted at the Institute of Innate Immunity at the University Hospital Bonn, Germany, under the supervision of Prof. Dr. Eicke Latz. It was designed by Prof. Dr. Eicke Latz, currently Professor of Experimental Rheumatology at Charité – Universitätsmedizin Berlin.

I carried out all experiments independently after being trained by Alesja Dernst (former PhD student, currently PostDoc, AG Latz, Bonn) and Romina Kaiser (Technician), except for the ChIP-sequencing and analysis of the H3K27 acetylation status. These experiments were conducted in collaboration with Sergi Cuartero (Junior Group Leader, Transcriptional Dynamics in Leukaemia Lab, Josep Carreras Research Institute, Barcelona, Spain), Lucia Lorenzi and Maria Cadefau-Fabregat (PhD students at the Josep Carreras Leukaemia Research Institute, Barcelona, Spain), who performed the ChIP-sequencing and the analysis of transcription factor binding sites.

I performed the statistical analysis independently under the guidance of Prof. Dr. Eicke Latz and Alesja Dernst.

In writing this thesis, I used DeepL and ChatGPT (version 3.5) to improve the readability, language, and spelling of the manuscript. After using these tools, I reviewed and edited the respective passages, and I take full responsibility for the content of the published dissertation.

I confirm that I wrote this dissertation independently and did not use any sources or resources other than those specified.

10 Publications

Parts of the contents of this dissertation have already been published in the following publication:

Wang, W, Dernst, A, Martin, B, Lorenzi, L, Cadefau, M, Phulphag, K, Wagener, A, Budden, C, Stair, N, Wagner, T, Färber, H, Jaensch, A, Stahl, R, Duthie, F, Schmidt, SV, Coll, RC, Meissner, F, Cuartero, S, Mangan, MSJ, Latz, E. Butyrate and propionate are microbial danger signals that activate the NLRP3 inflammasome in human macrophages upon TLR stimulation. Cell Rep 2024; 43: 114736

https://doi.org/10.1016/j.celrep.2024.114736

11 Acknowledgments

First of all, I would like to thank my supervisor, Prof. Dr. Eicke Latz, for giving me the opportunity to conduct the medical doctoral thesis at the Institute of Innate Immunity as part of the “Latzies”. During the past two years I have learnt a lot subject-related topics but also expanded my personal horizon. Thanks a lot for your support!

I am greatly indebted to Alesja Dernst, who provided me with outstanding support and excellent technical advice throughout the entire research time. I would also like to thank her for her great support during my laboratory work and for correcting the manuscript.

I would like to thank Dr. Matthew S. Mangan for his support and discussions about my project.

I would like to thank Dr. Wei Wang for kindly providing me with the topic and for the valuable discussions on this work. I would like to thank Theresa Wagner for being very helpful in the development of this project.

I would like to thank the technical assistant, Romina Kaiser, who was always available and helped me with answering questions, teaching me about monocyte purification and qPCR.

Many thanks to Dr. Dennis de Graf for all the conversations and encouragement during my study.

I would like to thank two close friends, Eva-Maria Staufenberg and Anne Marie Kaufmann, for always motivating and supporting me in most difficult times.

Finally, I would like to thank my father and my recently deceased mother, who supported me throughout my studies and gave me "roots and wings" in every situation in life.

I would like to thank everyone who has supported me in this work.